SYNTHESIS AND ELECTROPOLYMERIZATION OF NEW HYBRID MONOMERS CONTAINING CARBAZOLE UNITS

A THESIS SUBMITTED TO
THE GRADUATE SCHOOL OF NATURAL AND APPLIED SCIENCES
OF
MIDDLE EAST TECHNICAL UNIVERSITY

BY

MERVE AKBAYRAK

IN PARTIAL FULFILLMENT OF THE REQUIREMENTS
FOR
THE DEGREE OF MASTER OF SCIENCE
IN
CHEMISTRY

AUGUST 2016

Approval of the thesis:

SYNTHESIS AND ELECTROPOLYMERIZATION OF NEW HYBRID MONOMERS CONTAINING CARBAZOLE UNITS

Submitted by **MERVE AKBAYRAK** in partial fulfillment of the requirements for the degree of **Master of Science in Chemistry Department, Middle East Technical University** by,

Prof. Dr. Gülbin Dural Ünver _____
Dean, Graduate School of **Natural and Applied Sciences**

Prof. Dr. Cihangir Tanyeli _____
Head of Department, **Chemistry**

Prof. Dr. Ahmet M. Önal _____
Supervisor, **Chemistry Dept., METU**

Examining Committee Members:

Assoc. Prof. Dr. Ali Çırpan _____
Chemistry Dept., METU

Prof. Dr. Ahmet M. Önal _____
Chemistry Dept., METU

Assis. Prof. Dr. Görkem Günbaş _____
Chemistry Dept., METU

Prof. Dr. Atilla Cihaner _____
Chem. Eng. and Appl. Chem., Atılım Uni.

Assis. Prof. Dr. Demet Asil Alptekin _____
Chemistry Dept., METU

Date: 12.08.2016

I hereby declare that all information in this document has been obtained and presented in accordance with academic rules and ethical conduct. I also declare that, as required by these rules and conduct, I have fully cited and referenced all materials and results that are not original to this work.

Name, Last name: Merve AKBAYRAK

Signature:

ABSTRACT

SYNTHESIS AND ELECTROPOLYMERIZATION OF NEW HYBRID MONOMERS CONTAINING CARBAZOLE UNITS

Akbayrak, Merve

M.Sc; Department of Chemistry

Supervisor: Prof. Dr. Ahmet M. Önal

August 2016, 82 pages

This study consists of synthesis of alternating donor-acceptor type hybrid monomers based on various carbazole units as the electron rich donor group and thieno[3,4-c]pyrrole-4,6-dione (TPD) or 2,5-dihydro-3,6-di-2-thienyl-pyrrolo[3,4-c]pyrrole-1,4-dione (DPP) as the electron poor acceptor unit. The main goal of this research was not only to synthesize new low band gap polymers but also to shed more light on the substituent and linkage side effect of carbazole units on the optoelectronic properties of monomers and polymers. For this aim, four donor-acceptor-donor type monomers were synthesized via Suzuki coupling reaction and were characterized by spectroscopic techniques. The monomers synthesized in this work were polymerized by both potentiodynamic and potentiostatic electrochemical techniques. Electrochemically obtained polymer films, exhibited quasi-reversible redox behavior due to doping/dedoping of the polymers which were accompanied by a reversible electrochromic behavior. Their band gap values (E_g) were elucidate utilizing spectroelectrochemical and electrochemical data and it was found that polymers obtained from 3,6-substituted carbazole derivatives have slightly lower band gap values than 2,7-substituted carbazole derivatives.

Keywords: D-A-D approach, electrochromic polymers, carbazole, diketopyrrolo pyrrole dione, electrochemical polymerization.

ÖZ

KARBAZOL BİRİMLERİ İÇEREN YENİ HİBRİT MONOMERLERİN SENTEZİ VE ELEKTROKİMYASAL POLİMERİZASYONU

Akbayrak, Merve

Yüksek Lisans, Kimya Bölümü

Tez Yöneticisi: Prof. Dr. Ahmet M. Önal

Ağustos 2016, 82 sayfa

Bu çalışma karbazol birimlerinin elektronca zengin verici grup, tiyeno[3,4-c]pirol-4,6-diyon (TPD) veya 2,5-dihidro-3,6-di-2-tiyenil-pirolo[3,4-c]pirol-1,4-diyon (DPP) birimlerinin ise elektronca fakir alıcı grup olarak kullanılarak alternatif verici-alıcı-verici düzeninde yeni melez monomerlerin hazırlanması kapsamaktadır. Çalışmanın amacı düşük bant aralığına sahip yeni polimerler sentezlemenin yanı sıra karbazol birimindeki farklı birimler ve bağlanma pozisyonlarının etkileri ile farklı alıcı birim kullanılmasının monomerler ve polimerlerin optik ve elektronik özelliklerine etkilerini araştırmaktır. Bu amaçla Suzuki birleşme tepkimesi kullanılarak dört yeni verici-alıcı-verici tipi monomerler sentezlenmiş ve bu monomerlerin özellikleri, spektroskopik teknikler kullanılarak incelenmiştir. Monomerler, karakterizasyonları tamamlandıktan sonra, elektrokimyasal yöntemlerle polimerleştirilmiştir. Elde edilen polimer filmlerin yarı-tersinir redox özellik ve aynı zamanda tersinir elektrokromik özellik gösterdikleri gözlemlenmiştir. Yapılan spektroelektrokimyasal ve elektrokimyasal çalışmalar sonucunda 3,6 konumundan bağlı karbazol içeren polimerlerin 2,7 konumundan bağlı olanlara göre daha düşük bant aralığına sahip oldukları bulunmuştur.

Anahtar Kelimeler: D-A-D yaklaşımı, elektrokromik polimerler, karbazol, diketopirolo pirol diyon, tiyeno pirol diyon.

To my family,

especially to my spouse Serdar Akbayrak…

ACKNOWLEDGEMENT

I would like to express my deepest appreciation to my supervisor Prof. Dr. Ahmet M. Önal for his guidance, support, encouragement and patience. I am profoundly grateful to him for teaching me how to become a good scientist and for helping me in many ways. He was not only my supervisor but also a second father to me. It was an honor to work with him.

I would like to thank Assoc. Prof. Dr. Seha Tirkeş and Prof. Dr. Atilla Cihaner at Atılım University, Department of Chemical Engineering and Applied Chemistry, for his help and support.

I would like to thank to my laboratory collaborators Deniz Çakal and Elif Demir, for their kind friendship, support, patience and providing a perfect working enviroment. They made these years both funny and endurable.

Many thanks to Zeynep Ünal, Zühra Çınar, Ebru Özdemir for their beautiful friendship and sharing years together.

I am deeply grateful to Elif Gökçen Sakar for always being there for me. Since 2004, we grew up together and shared perfect moments. She is more than a sister for me.

Words fail to express my eternal gratitude to my family especially my spouse, Serdar Akbayrak, for believing in me and giving me endless support. Without their love, understanding and encouragement, I could not succeed anything. They made this life meaningful.

TABLE OF CONTENTS

ABSTRACT ..... **v**
ÖZ ..... **vii**
ACKNOWLEDGEMENT ..... **x**
TABLE OF CONTENTS ..... **xi**
LIST OF FIGURES ..... **xiii**
LIST OF SCHEME ..... **xvi**
LIST OF TABLES ..... **xvii**
ABBREVIATIONS ..... **xviii**
CHAPTERS
1. INTRODUCTION **1**
1.1. Brief History of Conducting Polymers 1
1.2. Conjugated Polymers 2
1.2.1. Band Gap Theory 3
1.2.2. Doping Process 5
1.2.3. Formation of Polaron and Bipolaron 7
1.2.4. Hopping process 8
1.3. Electrochromism In Conjugated Polymer 9
1.4. Synthesis of Conjugated Polymers 10
1.4.1. Chemical polymerization 10
1.4.2. Electrochemical polymerization 11
1.5. Coupling reactions 11
1.6. Overview of Carbazoles 13
1.7. Overview of Thieno Pyrrole Diones - TPD 15
1.8. Overview of Pyrrolo Pyrrole Diones - DPP 16
Aim of the Study 19
2.EXPERIMENTAL **21**
2.1. Materials and Measurement 21
2.2. Synthesis of Monomers 22

2.2.1. General procedure for the monomer synthesis 23
2.3. Synthesis of Polymers 25
2.4. Optical terms for characterization of polymers 27
2.4.1. Electrochromic contrast 27
2.4.2. Switching time 28
2.4.3. Coloration efficiency 28
3. RESULTS AND DISCUSSION 29
3.1. Structural Design of the Monomer 29
3.2. Properties of the Monomers 29
3.2.1. Properties of M1 29
3.2.2. Properties of M2, M3 and M4 31
3.3. Electrochemical Polymerization and Characteristics of the Polymers 39
3.3.1. Electrochemical Polymerization of M1 39
3.3.2. Optical and Electrochemical Characteristics of the PM1 40
3.3.4. Copolymerization of M1 with EDOT 42
3.3.5. Electrochemical Polymerization of M2, M3 and M4 51
3.3.6. Electrochemical Characteristics of the PM2, PM3 and PM4 55
3.3.7. Spectroelectrochemical and Switching Attitudes of the Polymers 58
3.3.8. Kinetic Studies and Switching Attitudes of the Polymers 63
3.3.9. FTIR Results of the Polymers 68
4. CONCLUSIONS 71
REFERENCES 73
APPENDIX 79

LIST OF FIGURES

Figure 1. 1. Chemical structures of some common conjugated polymers. 2

Figure 1. 2. Band gap illustrations for **a)** metals, **b)** semiconductors and **c)** insulators. 3

Figure 1. 3. Effects of conjugation on the band gap of conjugated polymer[17].....4

Figure 1. 4. Formation of new energy levels during doping and dedoping processes. 5

Figure 1. 5. Types of doping 6

Figure 1. 6. Conductivity range of conducting polymers and conductive polymeric composites.....6

Figure 1. 7. Band diagrams of bipolarons and polarons, in poly(heterocycles), showing the localized gap states and their occupancy. 7

Figure 1. 8. Electronic and chemical structural changes during (a) oxidation (p-doping) and (b) reduction (n-doping) of polyphenylene.[25] 8

Figure 1. 9. a) intramolecular and **b)** intermolecular hopping transport.....8

Figure 1. 10. Some examples of the electrochromic polymers. 9

Figure 2. 1. %T vs time graph.....27

Figure 3. 1. CV **(a)** and DPV **(b)** of **M1** in 0.2 M $TBABF_4$/DCM electrolytic solution. Inset: DPV of **A1**.....30

Figure 3. 2. Uv-Vis spectrum (solid line) and fluorescence spectrum (dash line) of **M1** in DCM (excitation at 350 nm). 31

Figure 3. 3. DPV of **(a) M2** (**b**) **M3** and (**c**) **M4** in 0.2 M $TBAPF_6$/DCM electrolytic solution. (Step Size 20 mV sample period, 1 s, pulse time 0.1 s and pulse size 25mV). 33

Figure 3. 4. (a) CV and **(b)** DPV of **A2** in 0.2 M $TBAPF_6$/DCM electrolytic solution (Step Size 20 mV sample period, 1 s, pulse time 0.1 s and pulse size 25mV for DPV). 34

Figure 3. 5. Uv-Vis spectra and PL spectra of (**a**) **M2**, (**b**) **M3** and (**c**) **M4** in DCM. Inset of (**a**), (**b**) and **(c)** are photographs of **M2**, **M3** and **M4** were taken under day light and UV lamp. (Excitation at 550 nm).....38

Figure 3. 6. Fluorescence emission spectra of **M3** in toluene, DCM and DMSO (Excited at 550 nm)..... 39
Figure 3. 7. (a) Absorbance spectrum of **PM1** in ACN on ITO coated glass and **(b)** spectroelectrochemistry of **PM1** film on an ITO coated glass in a monomer free 0.1 M ACN-$TBABF_4$ solution at applied potential range between -0.5 V and 1.2 V..... 41
Figure 3. 8. CV of **PM1** in 0.1 M ACN-$TBABF_4$ monomer free solution on ITO glass working electrode, at a scan rate of 20 $mV.s^{-1}$..... 41
Figure 3. 9. DPVs of **M1** and EDOT during their anodic scans 0.1 M DCM-$TBABF_4$. 43
Figure 3. 10. CVs of EDOT **(a)** and EDOT/**M1** monomer feed ratios of 9:1 **(b)**; 4:1 **(c)** and 1:1 **(d)** during electropolymerization on Pt WE between -0.8 V and 1.5 V in 0.1 M DCM-$TBABF_4$ with a scan rate of 100 $mV.s^{-1}$. The second **(e)** and the last **(f)** CVs of the electropolymerization cycles. **(g)** CVs of PEDOT and resulting copolymers in a monomer free solution containing 0.1 M $TBABF_4$ in ACN. 45
Figure 3. 11. The CVs of the copolymer (4:1) with increasing scan rate from 20 $mV.s^{-1}$ to 200 $mV.s^{-1}$ with 20 mV increments. (0.1 M DCM-$TBABF_4$ monomer free solution, on Pt working electrode vs Ag/AgCl). Inset: Variation of anodic and cathodic current densities vs voltage scan rate. 46
Figure 3. 12. Normalized electronic absorption spectra of the copolymer and homopolymer films in their neutral forms recorded in ACN. 47
Figure 3. 13. Electronic absorption spectra of PEDOT **(a) M1, (b)** copolymers of 9:1, 4:1, 1:1 **(c, d, e**, respectively) during potential scanning from -1.0 V to 1.0 V in 0.1 M ACN-$TBABF_4$ monomer free solution with scan rate of 20 $mV.s^{-1}$ and colors of homopolymers and copolymer (4:1) in their neutral and oxidized states **(f)**. (For **PM1**, potential scanning range is between -0.5 V and 1.2 V). 49
Figure 3. 14. CVs of copolymer and homopolymer films on ITO WE, recorded in 0.1 M ACN-$TBABF_4$ monomer free solution with scan rate of 20 $mV.s^{-1}$..... 51
Figure 3. 15. DPV of **(a) M2**, **(b) M3** and **(c) M4** with and without BFEE (Step Size 20 mV sample period, 1 s, pulse time 0.1 s and pulse size 25mV)..... 52
Figure 3. 16. Electropolymerization of the monomers **a) M2**, **b) M3**, and **c) M4** in 0.2 M $TBAPF_6$, BFEE: DCM (0.03:1-v:v) solution on a Pt disc electrode at 100 mVs^{-1} (50 cycle). Insets given in the figures represent the first cycles of CV..... 54

Figure 3. 17. Cyclic voltammograms of **(a) PM1**, **(b) PM2** and **(c) PM3** film in 0.1 M $TBABF_4$/ACN at scan rate of 200 mVs^{-1} 55
Figure 3. 18. Scan rate dependencies of electrochemically synthesized **(a) PM2**, **(b) PM3** and **(c) PM4** in 0.1 M $TBABF_4$/ACN at scan rates of 20-200 mV/s (Insets: Relationship of anodic and cathodic currents with respect to scan rate) 57
Figure 3. 19. Electronic absorption spectra of the polymers on ITO recorded in ACN containing 0.1 M $TBAPF_6$ as electrolyte between -0.5 and 1.0 V for **a) PM2**, **b) PM3** and between 0.0 and 1.2 V for **c) PM4**. Insets: CVs of polymer films recorded during spectroelectrochemical changes. 58
Figure 3. 20. Changes in the electronic absorption spectrum of **(a) M3** during controlled oxidation with $SbCl_5$ in DCM **(b) PM3** during controlled oxidation with $SbCl_5$ in o-dichlorobenzene **(c) PM3** during electrochemical oxidation on ITO in 0.1 M $TBAPF_6$/ACN.....62
Figure 3. 21. Chronoabsorptometry experiments for **PM2** on ITO in 0.1 M.....64
Figure 3. 22. Chronoabsorptometry experiments for **PM2** on ITO in 0.1 M.....65
Figure 3. 23. Chronoabsorptometry experiments for **PM3** on ITO in 0.1 M.....66
Figure 3. 24. FTIR spectra of **(a)** and **(b) M2** and **PM2, (c)** and **(d) M8** and **PM8**. 69

LIST OF SCHEME

Scheme 1. 1. Steps of catalytic cycle of crosscoupling reactions 12
Scheme 1. 2. General representation of Suzuki Coupling Reactions. 13
Scheme 1. 3. Substitution sites of carbazole 13
Scheme 1. 4. Types of carbazoles according to substitution sites 14
Scheme 1. 5. Schematic represantation of TPD 16
Scheme 1. 6. Schematic represantation of DPP 17
Scheme 2. 1. Suzuki coupling reaction for monomers. 22
Scheme 2. 2. Electrochemical polymerization of monomers. 26
Scheme 3. 1. Two steps reversible oxidation of A2. 35
Scheme 3. 2. Suggested mechanism for three step oxidation of **M4** 36
Scheme 3. 3. Radical coupling step of electro-oxidative polymerization for **M4** 36

LIST OF TABLES

Table 1. 1. Acceptors and donors used in this study 20
Table 3. 1. Electrochemical data of monomers and **A2** vs. Ag/ AgCl. 35
Table 3. 2. Electrochemical and optical properties of the copolymer films and homopolymer films. 50
Table 3. 3. Oxidation - reduction onsets and electronic band gap of **PM2**, **PM3** and **PM4** according to CV. 56
Table 3. 4. Optical band gaps of the polymers. 59
Table 3. 5. CE, switching time and colors of the polymers.....67

ABBREVIATIONS

E_g	Band Gap
CV	Cyclic Voltammogram
DPV	Differential Pulse Voltammogram
SPEL	Spectroelectrochemistry
ITO	Indium Tin Oxide
WE	Working Electrode
CE	Counter Electrode
RE	Reference Electrode
t	Time
ST	Switching Time
% T	Percent Transmittance
Δ%T	Percentage Transmittance Change
a.u.	Absorbance Unit
ACN	Acetonitrile
DCM	Dichloromethane
THF	Tetrahydrofuran
DMSO	Dimethylsulfoxide
$TBAPF_6$	Tetrabutylammonium Hexafluorophosphate
PEDOT	Poly(3,4-ethylenedioxythiophene)
D	Donor
A	Acceptor
D-A-D	Donor-Acceptor-Donor
HOMO	Highest Occupied Molecular Orbital
LUMO	Lowest Unoccupied Molecular Orbital
CE	Coloration Efficiency
TPD	Thieno pyrrole dione
DPP	Diketo pyrrolo pyrrole dione

CHAPTER 1

INTRODUCTION

1.1.Brief History of Conducting Polymers

Until Alan Heeger, Hideki Shirakawa and Alan MacDiarmid found that polyacetylene could conduct electricity upon doping, all carbon based polymers were known to be as insulators. In 1977 they reported that when silvery films of the semiconducting polymer, trans 'polyacetylene', $(CH)_x$ were exposed to chlorine, bromine, or iodine vapor, uptake of halogen occured, and the conductivity increased markedly (over seven orders of magnitude in the case of iodine) to give, silvery or silvery-black films, some of which have a remarkably high conductivity at room temperature.[1] This discovery open a new era in polymer chemistry and Alan Heeger, Hideki Shirakawa and Alan MacDiarmid were awarded with the Nobel prize in chemistry (2000) for showing how plastic can be transformed to conduct electricity. After this remarkable discovery, new classes of conducting polymers such as polythiophene, polypyrrole, polyaniline, poly(p-phenylene), poly(p-phenylenevinylene) and many others have been developed (Figure 1.1). [2]

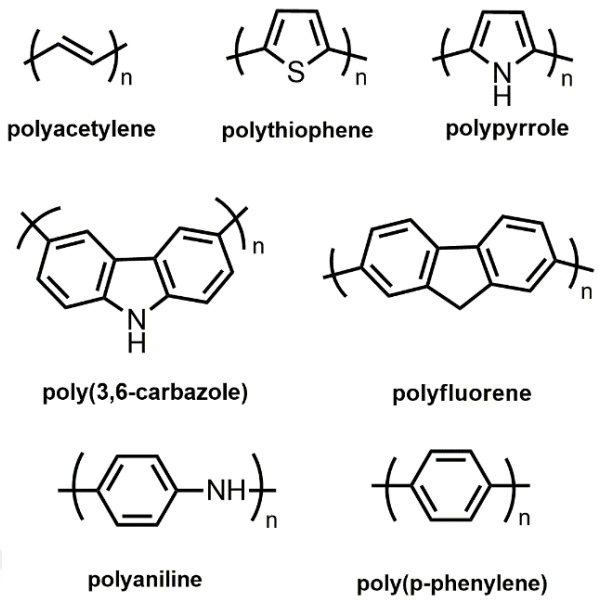


Figure 1. 1. Chemical structures of some common conjugated polymers.

1.2. Conjugated Polymers

A conjugated polymer chain consists of alternating single and double bonds, called conjugated double bonds. Double bonds, which are formed due to side to side overlap of p_z orbitals of carbon atoms, are called as π bonds and the π electrons are delocalized along the polymer chain. These delocalized π electrons fill up to whole band; therefore, conjugated polymers are intrinsic semiconductors.[3]

Conjugated polymers draw attention due to their ability to regulate the electronic and spectral properties such as easy band gap alternation and solution processability with chemical structural modifications.

Low-cost and easy manufacture of thin film devices are some of the basic advantages of organic semiconductors. High absorption coefficients of thin film make them good chromophores for optoelectronic applications. Addition, their high charge carrier mobilities make them competitive with amorphous silicon [4].

When explaining the conductivity of conjugated polymers, four factors could be mentioned;

1. Band gap theory
2. Doping process
3. Formation of polaron and bipolaron
4. Hopping process

1.2.1. Band Gap Theory

Highest occupied molecular orbital (HOMO), also known as the valence band (VB) and the lowest unoccupied molecular orbital (LUMO), known as the conduction band (CB) are the two discrete energy bands in conjugated polymers. The energy difference between these two bands is defined as the band gap (E_g) (Figure 1.2). [5]

The color, conductivity and optoelectronic properties of the conjugated polymers are affected by the E_g of molecule. Alternation of molecular weight,[6] bond length,[7] planarity,[8] aromatic resonance energy,[9] substituents,[10,11] and intermolecular attractions[12] are the factors that determine the E_g. In addition, donor-acceptor approach is highly important to change the band gap.[13]

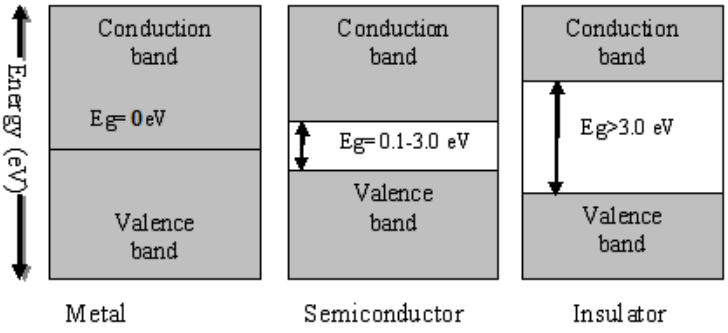


Figure 1. 2. Band gap illustrations for **a)** metals, **b)** semiconductors and **c)** insulators. [14]

In metals, there is no energy difference between conduction and valance bands. Therefore, E_g in metals is 0 eV.[15] Due to the overlapping of conduction and valance bands, metals always have partially filled free electron band. As a result, the electron can readily occupy the conduction band. The materials that have the band gap larger than 3.0 eV are called insulators because 3.0 eV is too high to promote electrons from valence band to the conduction band.[16] For semiconductors, on the other hand, the band gap value is between 0.0 and 3.0 eV.[14]

In the case of conjugated polymers repeating π orbitals along the chain form, the band structure and E_g of the conjugated polymers decrease with increasing conjugation length as shown in Figure 1.3. [17]

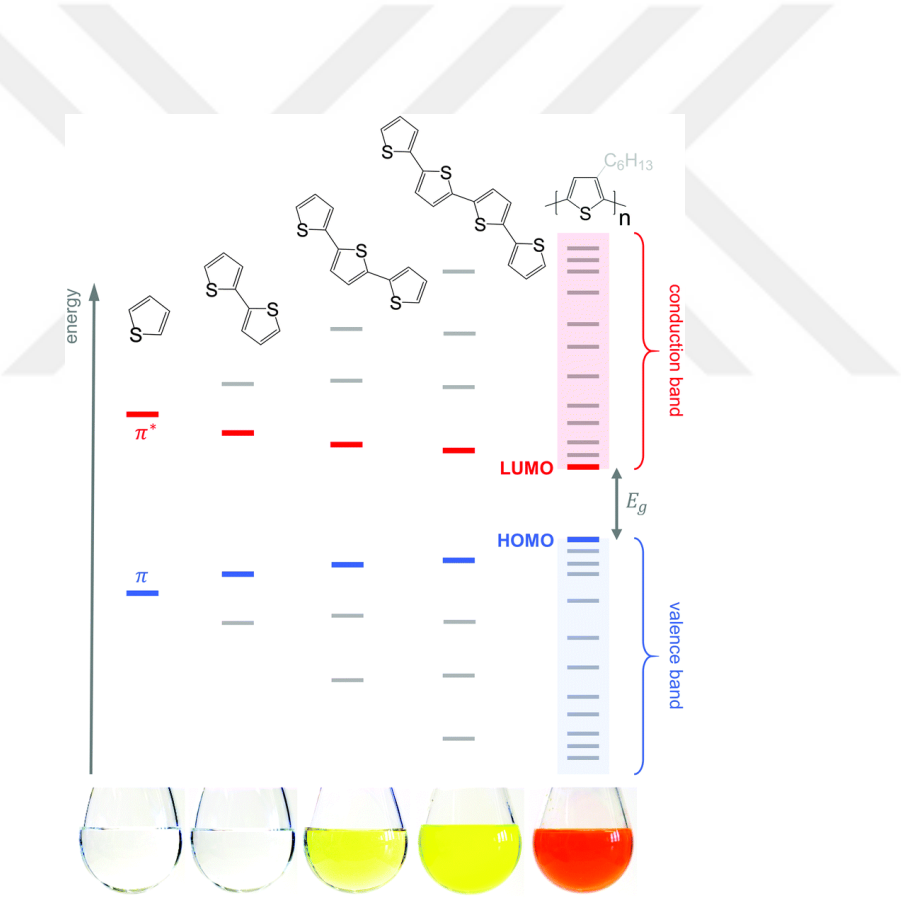


Figure 1. 3. Effects of conjugation on the band gap of conjugated polymer[17]

1.2.2. Doping Process

As it is known, conjugated polymers are semiconductors in their neutral states and their conductivities can be increased by doping process which can be achieved by both chemical or electrochemical ways. This process allows controlling the optoelectronic properties of conjugated polymers.

The doping of conjugated polymers implies;

(i) the charge transfer (by oxidation, p-type, or reduction, n-type),
(ii) the insertion of a counter ion (to neutralize the overall charge),
(iii) the simultaneous control of the Fermi level.[18]

In doping process, removing (oxidation) or inserting an electron (reduction) forms new energy levels between valance and conduction bands which cause a decrease in the effective band gap of conjugated polymers (Figure 1.4).[18] According to their dopant counter ions, polymers are classified as n-doped (reduced) and p-doped (oxidized) (Figure 1.5). p-doping process has been encountered more frequently as compared to the n-doping process due to the requirement of ultra dry and oxygen-free conditions for n- doping process. [19]

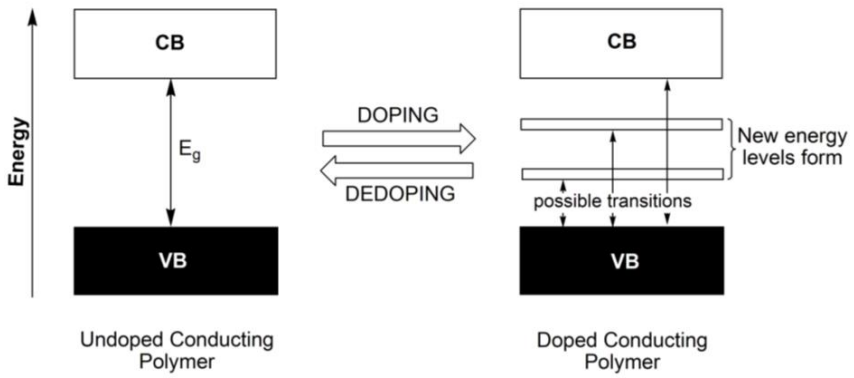


Figure 1. 4. Formation of new energy levels during doping and dedoping processes.

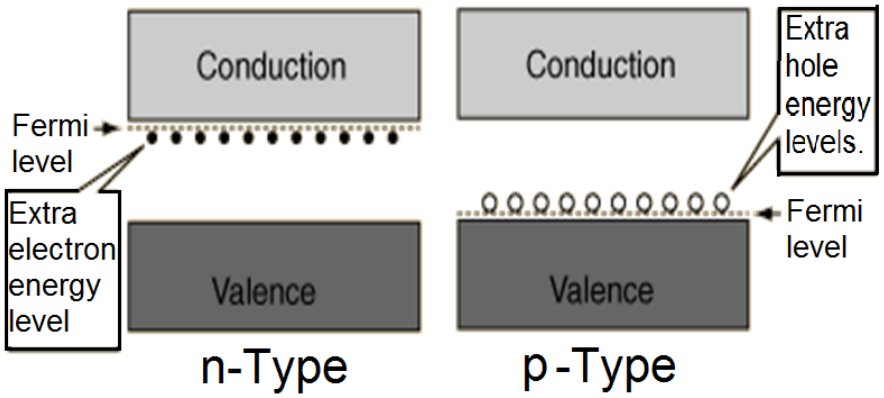


Figure 1. 5. Types of doping [20]

During the doping process, radical cations or anions (positive/negative polarons) are generated, which are delocalized in the polymer backbone and provide conductivity. Generally, the conductivity of conjugated polymers in their neutral state is very low, in the order of 10^{-4}–10^{-9} S cm^{-1}. However when they are doped, their conductivities can be increased up to that of metallic conductors (Figure 1.6).[21]

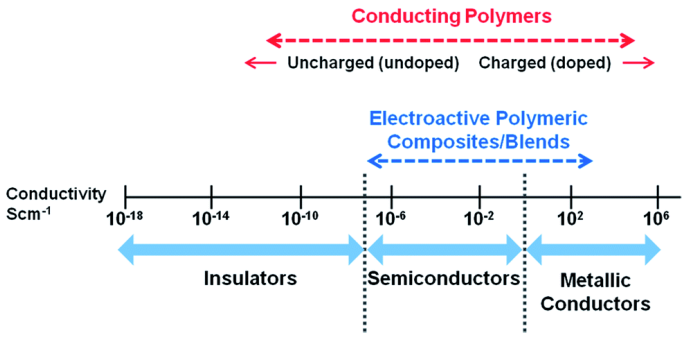


Figure 1. 6. Conductivity range of conducting polymers and conductive polymeric composites

1.2.3. Formation of Polaron and Bipolaron

Polarons are radical cations or anions formed upon oxidation, or reduction, respectively. These species act as charge carriers (Figure 1. 8) in an applied electric field. Polaron formation creates new localized electronic states in the band gap as shown in Figure 1.7. [22]

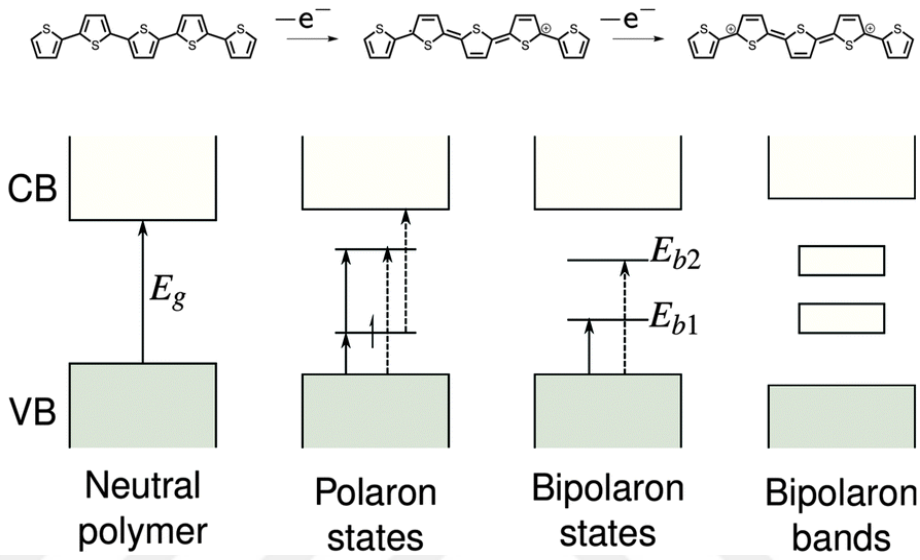


Figure 1. 7. Band diagrams of bipolarons and polarons, in poly(heterocycles), showing the localized gap states and their occupancy.[23]

Bipolarons, on the other hand, are formed upon further oxidation or reduction of polymer chain.[24]

Formation of polarons and bipolarons as a result of p- or n-doping is examplified in Figure 1.8 for polyphenylene. A radical cation (positive polaron) is formed via oxidation, while a radical anion (negative polaron) is formed during reduction. High states of charge can lead to the formation of positive and negative bipolarons. Cations and anions counter balance charges in the polymer chain. [25]

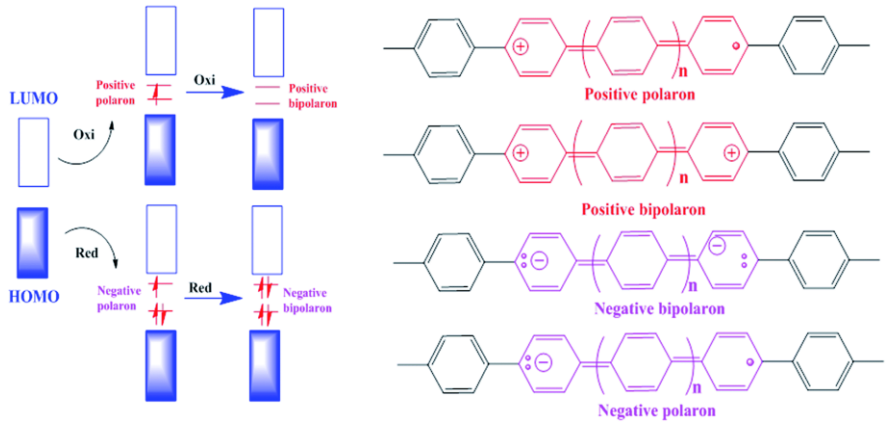


Figure 1. 8. Electronic and chemical structural changes during (a) oxidation (p-doping) and (b) reduction (n-doping) of polyphenylene.[25]

1.2.4. Hopping process

The overall mobility of charge carriers in conducting polymers depends on two components; intra-chain and inter-chain charge transfer (Figure 1.9). In intra-chain mobility, the charge transfer occurs along the polymer chain. Because of the high molecular weight of conducting polymer chains, the conductivity is supplied by interchain hopping which is dependent on the interchain π-π stacking.[26] The interchain interactions may provide better stacking between the chains or cause electron transitions from π-band of one chain to the π-band of another chain. However the interchain interactions are significantly weaker than the intra-chain π-electron interactions.[27]

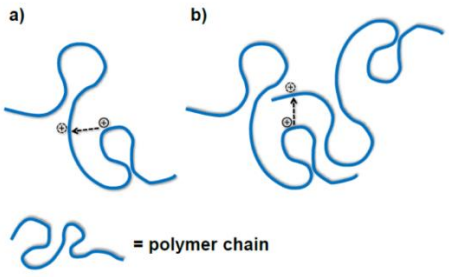


Figure 1. 9. a) intramolecular and **b)** intermolecular hopping transport

1.3. Electrochromism in Conjugated Polymers

Conjugated polymers are mostly electrochromic and they have several advantages such as color tunability, high optical contrast, fast switching speed, and processability.[28] Electrochromism can be defined as reversible, persistent and visible color changes in a conjugated polymer system and which is observed upon external potential.[29] Electrochromic polymers can be used in many applications such as smart windows, displays, and data-storage devices.[30] Figure 1.10 shows a series of electrochromic soluble polymers spray-cast onto ITO-coated glass in their neutral and doped states.

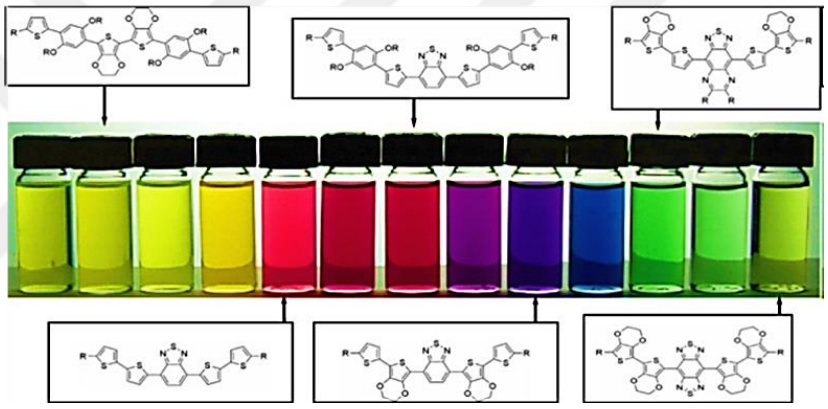


Figure 1. 10. Some examples of the electrochromic polymers.[31]

Some of the main advantages of conjugated polymers are:

i. high coloration efficiency,
ii. good mechanical properties,
iii. ease of colour tuning via structural modifications,
iv. low switching times,
v. low cost,
vi. ease of processing.

Among them, the ease of colour tuning is one of the most desired properties. In the literature, there are many researches related with the expansion of the "colour palette" of electrochromic conjugated polymers. In these research several different approaches have been investigated:

- modification of the HOMO and LUMO energy levels of the building blocks in the repeating unit,
- alternation of the backbone planarity (π-overlap),
- increase of the conjugation length,
- use of a donor–acceptor approach in the repeating unit.[32]

1.4. Synthesis of Conjugated Polymers

Chemical and electrochemical polymerizations are two of the most common ways to synthesize conjugated polymers.

1.4.1. Chemical polymerization

Synthesis of conjugated polymers can be achieved either via oxidative reaction or, especially in the synthesis of donor acceptor type polymers, coupling reactions. Oxidative polymerization is one of the least expensive, simplest, and the most widely used ways of synthesizing conducting polymers.[33] In oxidative polymerizations, oxidizing agent such as ferric chloride ($FeCl_3$), ammonium peroxydisulfate ($(NH_4)_2S_2O_8$), potassium permanganate ($KMnO_4$) are used to produce polymer in its doped or conducting form. Reduction to the neutral state is accomplished by the addition of strong base such as ammonium hydroxide or hydrazine. Chemical polymerization takes place in the bulk of the solution, and the resulting polymers precipitate as insoluble solids having limited degree of polymerization. If strong oxidizing agents are used, overoxidation and decomposition may also occur.[34]

1.4.2. Electrochemical polymerization

In the electrochemical polymerization, a coupling occurs between two electrolytically initiated radical cations or anions. The radical cation reacts with another radical cation to yield a neutral dimer by the loss of two protons. The oxidized dimer radical cation again attacks to form a trimer and the propagation proceeds to form polymer. Electropolymerization proceeds then through successive electrochemical and chemical steps, until the oligomer becomes insoluble in the electrolytic medium and precipitates onto the electrode surface.[35]

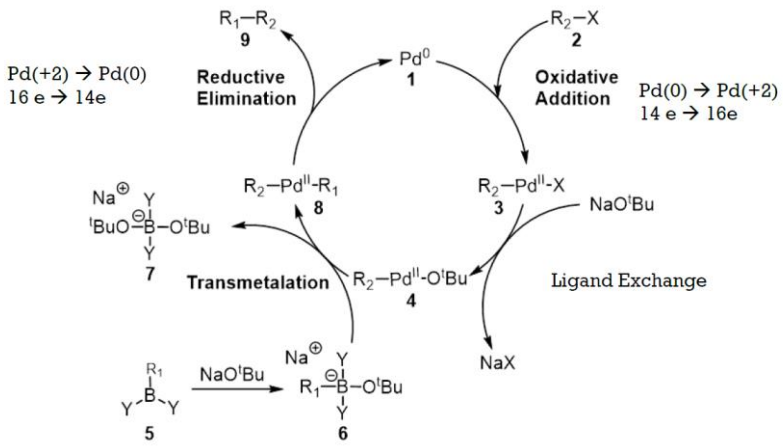
Electrochemical polymerization is commonly carried out employing one of three techniques. These methods involve the application of (i) a constant potential (potentiostatic), (ii) a variable current and voltage (potentiodynamic) and (iii) a constant current (galvanostatic).[36] To carry out electropolymerization, a three electrode system is required. These electrodes are known as counter electrode, reference electrode and working electrode. The electrochemically synthesized polymer is deposited onto the working electrode which can be a platinum, glassy carbon or indium tin oxide (ITO).[37] The advantages of electrochemical polymerization over the chemical polymerization can be given as follows:

i. Reaction can be conducted at room temperature.
ii. Homogeneous polymer thin films can be directly med on electrode surface.
iii. Film thickness can be controlled.
iv. Doping process can be performed at the same time during the formation of thin film.
v. There is no need of purification.
vi. Copolymers can be obtained easily.

1.5. Coupling reactions

Palladium-mediated cross-coupling reactions are attractive organometallic transformations for the generation of C--C, C--N, C--O, and C--S bonds.[38]

A general catalytic cycle for the cross-coupling reaction of organometallics, which involves oxidative addition-transmetalation-reductive elimination steps, is shown in Scheme 1.1 and the steps explained via diagram.[38]



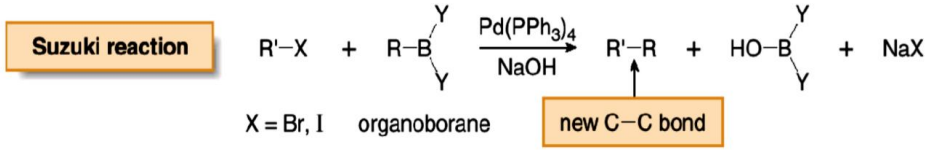
Oxidative addition	Transmetallation	Reductive elimination
• The rate determining step of the catalytic cycle • Couples the palladium catalyst to the alkyl halide which gives rise to the organopalladium complex • The complex is initially in the cis conformation but isomerizes to the trans conformation • Stereochemistry with vinyl halides are retained but inversion of stereochemistry occurs with allylic or benzylic halides	• The role of base is to activate the boron-containing reagent, and also facilitate the formation of R_1Pd-OR from R_1Pd-X. • Reaction does not occur in the absence of base. • Exact mechanism is unclear.	• This final step gives the desired product and it also regenerates the palladium catalyst so that it can participate again in the catalytic cycle (ie. Making more products). • Require the complex to revert back to the cis conformation before reductive elimination can occur

Scheme 1. 1. Steps of catalytic cycle of crosscoupling reactions[39]

Among coupling reactions, Suzuki coupling reaction is a highly preffered coupling reaction among the others due to its several advantages such as

- Mild reaction conditions
- Availability of common boronic acids
- Easily removing of inorganic by-products
- Less toxicity of boronic acids compared to organostannanes.[40]

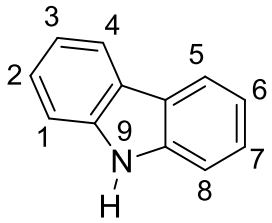
Formation of C-C bond via Suzuki coupling reaction is shown schematically in Scheme 1.2.



Scheme 1. 2. General representation of Suzuki Coupling Reactions.

1.6.Overview of Carbazoles

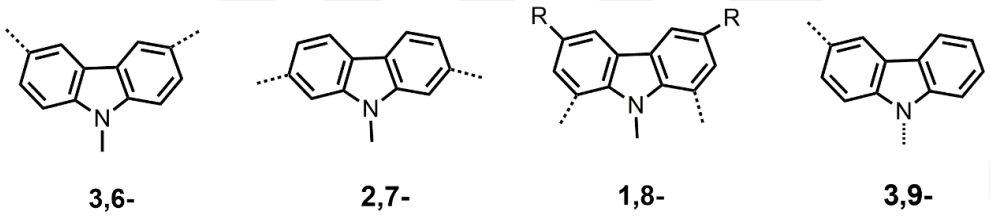
Carbazole is a biphenylene system with a nitrogen bridge as shown in Scheme 1. 3. It is a tricyclic fused aromatic compound having pyrrole in the middle of the compound and two fused benzene rings to pyrrole. The nitrogen behaves as an ortho-, para-directing activating unit, and undergoes electrophilic substitution at the 3,6-position first. [41]



Scheme 1. 3. Substitution sites of carbazole

In view of the electron donating effects of the nitrogen, the polycarbazoles possess higher HOMO energy levels than the polyfluorenes, which can improve their charge injection and transport properties. Because of these properties, carbazoles are more preferred than fluorenes for optoelectronic applications such as transistors and LEDs. Moreover, as oppose to polyfluorenes, polycarbazoles are of particular interest for blue-emitting for LEDs as they cannot produce green-emitting ketone defects through oxidation.[42]

When the linkage side is considered, there are four types of carbazoles; 3,6-, 1,8-, 2,7- and 3,9-substituted carbazoles (Scheme 1. 4). Among them only 2,7-linked carbazoles retain conjugation. For the others, conjugation can only go through the nitrogen bridgehead atom.[49]



Scheme 1. 4. Types of carbazoles according to substitution sites

Carbazole has many advantages to be used in optoelectronic applications[43,44] and some of them are listed below:

(1) 9*H*-carbazole is a cheap raw material.
(2) The nitrogen atom can be easily functionalized with a large variety of substituents to modulate the carbazole properties without increasing the stericinteractions near the backbone.
(3) Carbazole units can be linked at different positions.
(4) Due to the fully aromatic configuration of carbazole which exhibit good chemical, thermal, photochemical and environmental stabilities.
(5) It has high charge carrier stability.

Among various classes of conjugated polymers, polycarbazole derivatives are of great importance because of its variety of useful properties, such as easy formation of relatively stable radical cations (holes), high charge carrier mobility, and high thermal and photochemical stability[14-18]. Moreover, homopolymers of carbazoles exhibit blue fluorescence with a maximum of emission near 415-440 nm with relatively high quantum yields.[45] These properties make polycarbazole derivatives as suitable materials for optoelectronic applications.

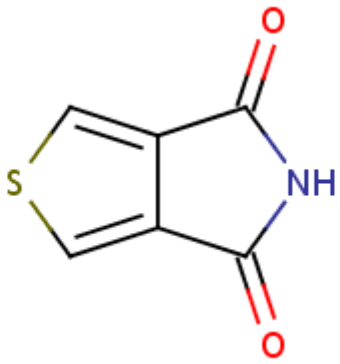
There are a large number of reports showing the advantages, disadvantages, interesting electrochromic properties and differences of 3,6-linked and 2,7-linked carbazoles in literature. Data and coworkers demonstrated the effect of the different linkages of carbazole groups in electroactive monomers and their corresponding electropolymers on their photochemical and electrochemical properties. They found that 3,6- linked carbazole derivatives are more stable under electrochemical conditions than their 2,7-linked analogues.[46]

Recently, low bandgap copolymers containing carbazole and diketopyrrolopyrrole units have been prepared independently by Leclerc[47,48] and by Hashimoto and co-workers.[49] The optical band gaps were estimated from onset of absorption bands and are reported to be around 1.60 eV.

1.7.Overview of Thieno Pyrrole Diones-TPD

Thieno[3,4-c]pyrrole-4,6-dione (TPD) (Scheme 1. 5) has received great attention as electron poor acceptor unit in synthesizing donor acceptor types polymers. TPD has relatively simple, compact, symmetric, and planar structure. These structral characteristic can be beneficial for electron delocalization when it is incorporated into various conjugated polymers. TPD greatly lowers the HOMO-LUMO energy levels due to the the strong electron-withdrawing imide of TPD.[50] Moreover, TPD promote interchain and intrachain interactions along the polymer chains.[51] TPD can also gain some

stabilization energy by forming a quinoidal thiophene-maleimide structure in its excited state, it is possible to afford a polymer with low energy band gap.[52]

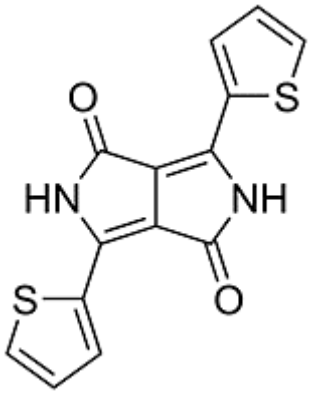


Scheme 1. 5. Schematic represantation of TPD

Tian research group has synthesized three donor–acceptor (D–A) copolymers containing 1,3-di(thien-2-yl)thieno[3,4-c]pyrrole-4,6-dione acceptor unit and different donor units including fluorene, 2,7-carbazole and benzodithiophene in 2012. They reported that optical band gap of carbazole and fluorene containing copolymers were 2.30 and 2.28 eV, respectively. Moreover, intramolecular charge transfer was found to be lower for carbazole and fluorene than that of benzodithiophene anologues.[53]

1.8. Overview of Pyrrolo Pyrrole Diones – DPP

2,5-Dihydro-3,6-di-2-thienyl-pyrrolo[3,4-c]pyrrole-1,4-dione (DPP) unit contains two fused lactam rings which lead to strong π-π interaction (Scheme 1. 6). The electron deficient lactam rings make the DPP unit to exhibit strong electron-withdrawing effect. Moreover, the well conjugated structure leads to strong π-π interaction and causes strong absorption in the visible and even the near-infrared region (from about 700 nm to 2500 nm).[50,54]



Scheme 1. 6. Schematic represantation of DPP

Strong electron deficient characteristic of DPP unit combined with high planarity and aggragation allows to absorb in the near IR region and exhibit good electron and hole mobilities. The use of thiophene flanking unit also promotes a more coplanar backbone. Not only planar structure but also very strong push pull effect of the electron rich donor and the electron deficient DPP core decrease the band gap of thiophene containing polymer.[55]

The most important advantages of DPP derivatives are listed below;

i. They can undergo several synthetic modifications.
ii. They can act as a strong acceptor unit.
iii. They exhibit high fluorescence quantum yield.
iv. They possess high thermal and photostability.

These properties make DPP an excellent building block for many applications.[56] Furthermore, its polar nature enhances the crystallization tendency of polymers. As a result, DPP based conjugated polymers show broad and tunable optical absorption, up to 1000 nm, and high hole and electron mobility which can result in a high photo current and good fill factor in solar cells.[57]

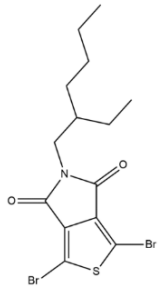
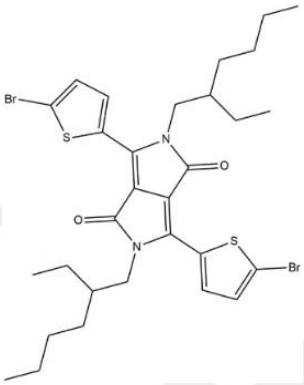
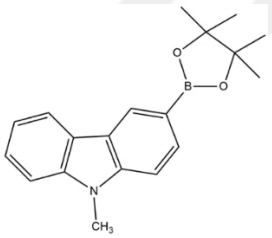
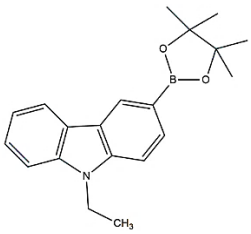
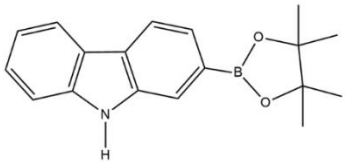
Recently, the synthesis of DPP containing polymers have been arised dramatically.[58] Due to several attractive properties of diketopyrrolopyrrole (DPP) dyes for photovoltaic applications, such as strong light absorption, good photochemical stability, and facile synthetic modification, Christian B. *et al*. reported the properties of a large number of DPP containing polymers in their review.[59]

Zhou *et al*. synthesized several diketopyrrolopyrrole-based donor-acceptor (D-A) type copolymers containing fluorene, carbazole and dithienopyrrole as donor unit were presented in their study. They found the optical band gap 1.75 eV, 1.63 eV, and 1.13 eV for fluorene, carbazole and dithienopyrrole containing copolymer, respectively and also similar trend was found for electronic band gap of the copolymers.[49]

Aim of the Study

In this study, our aim is to design and synthesize new DAD type monomers and polymers to elucidate more information on the substituent and linkage site effect of carbazole units on the optoelectronic properties of carbazole based molecules. For this purpose, various carbazole units as the electron rich donor group and thieno[3,4-c]pyrrole-4,6-dione (TPD) or 2,5-dihydro-3,6-di-2-thienyl-pyrrolo[3,4-c]pyrrole-1,4-dione (DPP) as the electron poor acceptor unit (Table 1. 1) were used. These donor and acceptor units were coupled via Suzuki coupling reaction to obtain the monomers; *5-(2-ethylhexyl)-1,3-bis(9-methyl-9H-carbazol-3-yl)-4H-thieno[3,4-c]pyrrole-4,6(5H)-dione* (**M1**), *2,5-bis(2-ethylhexyl)-3,6-bis(5-(9-methyl-9H-carbazol-3-yl)thiophen-2-yl)pyrrolo[3,4-c]pyrrole-1,4(2H,5H)-dione*(**M2**), *3,6-bis(5-(9-ethyl-9H-carbazol-3-yl)thiophen-2-yl)-2,5-bis(2-ethylhexyl)pyrrolo[3,4-c]pyrrole-4(2H,5H)-dione* (**M3**), *2,7-bis(5-(9H-carbazol-2-yl)thiophen-2-yl)-2,5-bis(2-ethylhexyl)pyrrolo[3,4-c]pyrrole-1,4(2H,5H)-dione* (**M4**) (Scheme 2. 1). After characterization of monomers, their corresponding polymer films, *poly (5-(2-ethylhexyl)-1,3-bis(9-methyl-9H-carbazol-3-yl)-4H-thieno[3,4-c]pyrrole-4,6(5H)-dione)* (**P1**), *poly(2,5-bis(2-ethylhexyl)-3,6-bis(5-(9-methyl-9H-carbazol-3-yl)thiophen-2-yl)pyrrolo[3,4-c]pyrrole-1,4(2H,5H)-dione)*(**P2)**, poly(*3,6-bis(5-(9-ethyl-9H-carbazol-3-yl)thiophen-2-yl)-2,5-bis(2-ethylhexyl)pyrrolo[3,4-c]pyrrole- ,4(2H,5H)-dione)* (**P3**),*poly*(*2,7-bis(5-(9H-carbazol-2-yl)thiophen-2-yl)-2,5-bis(2-ethylhexyl)pyrrolo[3,4- c]pyrrole-1,4(2H,5H)-dione)*(**P4**) were obtained by electrochemical polymerization techniques (Scheme 2. 2). The electrochemical and optical properties of polymers were investigated in terms of type of substituent and linkage site utilizing electroanalytical and spectroscopic techniques.

Table 1. 1. Acceptors and donors used in this study

	1,3-dibromo-5-(2-ethylhexyl)-4H-thieno[3,4-c]pyrrole-4,6(5H)-dione **A1- (TPD)**
	3,6-bis(5-bromothiophen-2-yl)-2,5-bis(2-ethylhexyl)pyrrolo[3,4-c]pyrrole-1,4(2H,5H)-dione **A2- (DPP)**
	9-methyl-9H-carbazole-3-boronic acid pinacol ester **D1**
	9-ethyl-9H-carbazole-3-boronic acid pinacol ester **D2**
	9H-carbazole-2-boronic acid pinacol ester **D3**

CHAPTER 2

EXPERIMENTAL

2.1. Materials and Measurement

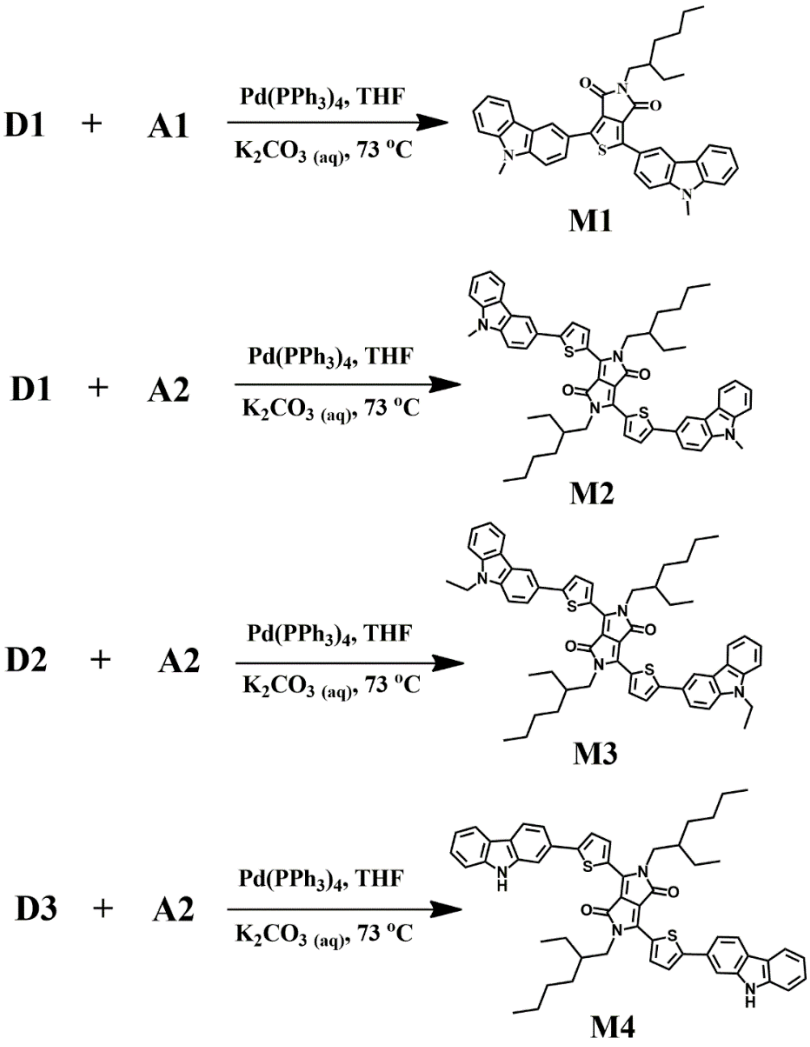
All chemicals were purchased from Sigma Aldrich Chemicals except **A2**, was purchased from Derthon Chemicals, and used as received unless otherwise noted. Acetonitrile (ACN) and dichloromethane (DCM) were distilled and purged with nitrogen before use. Tetrahydrofuran (THF) were dried over Na/benzophenone ketyl and freshly distilled. Electrochemical studies were performed by using a platinum (Pt) disc as a working electrode (WE), a Pt wire as a counter electrode (CE) and a silver-silver chloride (Ag/AgCl) (in 3 M NaCl(aq) solution) as a reference (RE) electrode. The cyclic voltammograms (CV) were recorded with Gamry Reference 300 model potentiostat-galvanostat. The differential pulse voltammograms (DPV) were also recorded with Gamry Reference 300 model potentiostat-galvanostat by applying 20mV step size, 1 s sample period, 0.1 s pulse time and 25mV pulse size. Spectroelectrochemical measurements were performed using a Carry 60 model UV-VIS spectrometer combined with Gamry Reference 300 potentiostat–galvanostat. Indium tin oxide (ITO, Delta Tech. 8 – 12 Ω, 0.7 cm × 5 cm) coated glass, a Pt wire and a Ag wire were used as WE, CE, and pseudo RE, respectively. Fluorescence measurements were recorded on a Varian Cary Eclipse Fluorescence Spectrophotometer.

Structural characterization of the monomer was revealed by using ^{1}H and ^{13}C NMR spectra, recorded on a Bruker Spectrospin Avance DPX-400 Spectrometer in $CDCl_3$ at 400 MHz. Chemical shifts were calculated relative

to tetramethylsilane (TMS) as the internal standard during measurements. FT-IR analysis of the monomers and polymers were performed with Thermo Scientific Nicolet S10 with attenuated total reflectance. All measurements were performed at room temperature under ambient conditions.

2.2. Synthesis of Monomers

Synthesis of the monomers were achieved via Suzuki coupling reaction as shown in Scheme 2. 1.



Scheme 2. 1. Suzuki coupling reaction for monomers.

2.2.1. General procedure for the monomer synthesis

Acceptor (0.3 mmol), donor (0.6 mmol), and 5% of Pd (0) were dissolved in freshly distilled THF (20.0 mL) and stirred under nitrogen gas (N_2) for 15 min. Potassium carbonate (K_2CO_3) (10.0 mmol) was dissolved in 5.0 mL distilled water and degassed for 10 min. Then, 1.0 mL of aqueous K_2CO_3 solution was added to the reaction mixture. The mixture was purged with N_2 for 30 min, and refluxed for 48 h at 73ºC. The progress of reaction was monitored by using thin layer chromatography (TLC) and the reaction was stopped after 48 h. THF was removed under reduced pressure and the crude product was extracted with DCM. The combined organic layers were washed with brine, dried ($MgSO_4$), and concentrated *in vacuo*. Further purification was done by using silica gel column chromatography; for **M1** 3 DCM: 1 Hexane solvent system was used and final product was obtained as yellow solid (120 mg, 64%), for **M2, M3** and **M4** 6 Hexane: 2 DCM: 1 Ethyl acetate: 1 Chloroform solvent system was used and recrystallization was done with 20 Hexane: 1 DCM. Final products were obtained as blue solid.

M1

^{1}H NMR ($CDCl_3$) d: 8.82 ppm (s, 2H), 8.32 ppm (d, 2H), 8.20 ppm (d, 2 H), 7.49 ppm (t, 2H), 7.345 ppm (t, 4H), 7.28 ppm (t, 2H), 5.29 ppm (s, 6H), 3.61 ppm (d, 4H), 1.92 ppm (m, 2H), 1.32 ppm (m, 16H), 0.9 ppm (t, 6H), 0.88 (t, 6H). (See appendix A. 1)

^{13}C NMR ($CDCl_3$) d: 163.73, 145.7, 141.71, 141.56, 128.45, 126.33, 126.25, 123.09, 122.87, 122.130, 120.80, 120.40, 119.64, 108.768, 108.58, 53.40, 38.24, 31.6, 29.24, 23.97, 22.65, 14.1, 10.6 ppm.

M2

^{1}H NMR: (400 MHz, $CDCl_3$) δ (ppm) : 9.03 (d, 2H), 8.39 (s, 2H), 8.17 (d, 2H), 7.82 (d, 2H), 7.53 (m, 4H), 7.44 (d, 4H), 7.30 (d, 2H), 4.15 (dd, 4H), 3.89 (s, 6H), 2.03 (m, 2H), 1.53 (m, 8H), 1.4 (h, 4H), 1.29 (m, 4H), 0.9 (t, 6H), 0.85 (t, 6H). (See appendix A. 2)

HRMS calculated for $C_{56}H_{58}N_4O_2S_2$: 882.4001. Found 882.4067

M3

^{1}H NMR: (400 MHz, $CDCl_3$) δ (ppm): 9.04 (d, 2H), 8.41 (d, 2H), 8.17 (d, 2H), 7.82 (d, 2H), 7.52 (t, 4H), 7.46 (d, 4H), 7.29 (d, 2H), 4.4 (q, 4H), 4.15 (d, 4H), 2.05 (m, 2H), 1.55 (m, 8H), 1.42 (t, 6H), 1.31 (h, 4H), 1.25 (m, 4H), 0.96 (t, 6H), 0.90 (t, 6H). (See appendix A. 3)

HRMS calculated for $C_{58}H_{62}N_4O_2S_2$: 911.4392. Found 911.4406

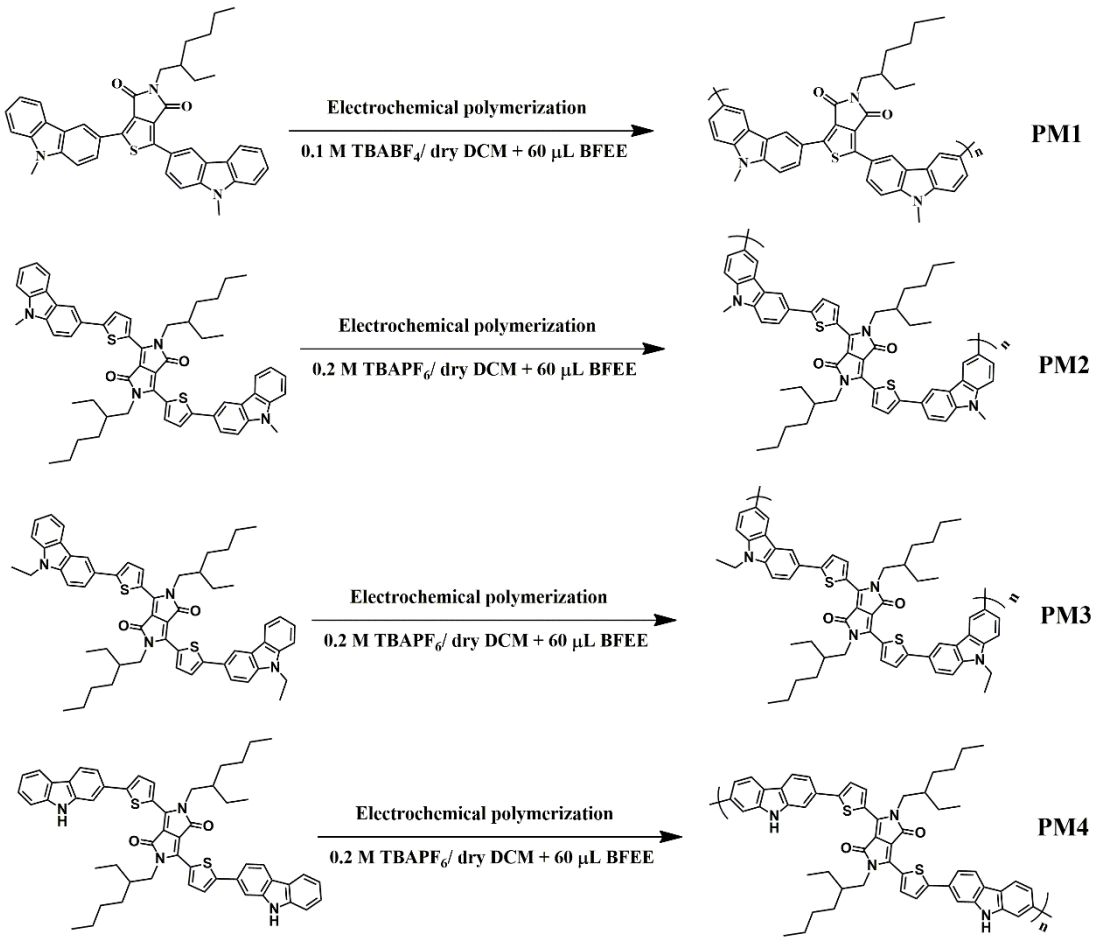
M4

^{1}H NMR: (400 MHz, C_2D_6OS) δ (ppm): 11.4 (s, 2H), 8.91 (d, 2H), 8.22 (d, 2H), 8.17 (d, 2H), 7.92 (d, 2H), 7.88 (s, 2H), 7.64 (d, 2H), 7.52 (d, 2H), 7.43 (t, 2H), 7.20 (t, 2H), 4.09 (q, 4H), 1.88 (m, 2H), 1.33 (m, 8H), 1.23 (m, 8H), 0.9 (t, 6H), 0.83 (t, 6H). (See appendix A. 4)

HRMS calculated for $C_{54}H_{54}N_4O_2S_2$: 855.3766. Found 855.3765.

2.3. Synthesis of Polymers

In this work, all monomers were polymerized via electrochemical methods. The electrochemical polymerization of the monomers were achieved in an electrolyte solution consisting of 0.2 M $TBAPF_6$ dissolved in dry DCM and 60 μL borontrifluoride diethyl etherate (BFEE). Polymer films were obtained on the WE surface either by potential cycling or constant potential electrolysis.For the analysis of polymer films, monomer-free electrolytic solution including ACN and 0.1 M $TBABF_4$ was used.



Scheme 2. 2. Electrochemical polymerization of monomers.

2.4. Optical terms for characterization of polymers

2.4.1. Electrochromic contrast

Electrochromic contrast is measured as the percent transmittance change (ΔT) of the electrochromic material in other words transmittance difference between the redox states of a polymer at a specific wavelength and it is an essential parameter for characterizing the electrochromic materials. Equation 1-1 shows the calculation of percent transmittance. It can be calculated by extracting the percent transmittance of bleached state and that of colored state in a redox cycle (Figure 2. 1)

$$\Delta\%\ T = (\%\ T_{bleached}) - (\%\ T_{colored}) \qquad \text{(Equation 2-1)}$$

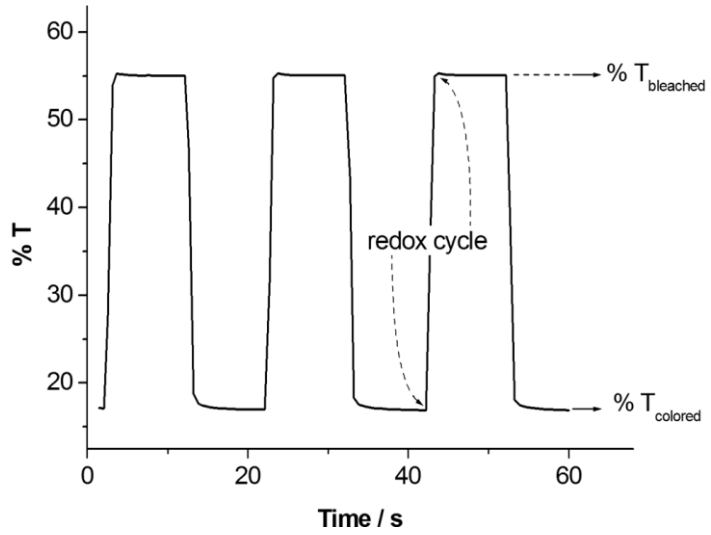


Figure 2. 1 %T vs time graph[60]

For applications such as smart windows the difference between the bleached and colored states is expected to be the highest. To convey more information on the perception of transmittance to the human eye, measurements on the relative luminance change during an electrochromic switch are also considered to be useful. [59]

2.4.2. Switching time

Switching time (response time) is defined as the time required to switch between the two extreme redox states of the electrochromic material. It is generally followed by a square wave potential step method coupled with optical spectroscopy. [61]

2.4.3. Coloration efficiency

Coloration efficiency (CE), which basically defines the change in optical density per injected charge, is a fundamental parameter for investigating the power requirements of electrochromic materials.[62]

Coloration efficiency is the parameter of optical density while polymer is doped and dedoped. Generally it is assigned as η and has cm^2/C unit. It is calculated with tandem chronocoulometry / chronoabsorptometry measurements. In order to calculate coloration efficiency, firstly optical density (Δ OD) should be calculated (Equation 2-2).[63]

$$\Delta OD = \log (T_{bleached} / T_{colored}) \qquad \text{(Equation 2-2)}$$

$$\eta = \Delta OD / Q \qquad \text{(Equation 2-3)}$$

CHAPTER 3

RESULTS AND DISCUSSION

3.1. Structural Design of the Monomers

The aim of this study was to synthesize new donor-acceptor-donor types homopolymers to obtain low band gap and high optical contrast. Moreover, it was intended to investigate the effect of different donor and acceptor units on the electrochemical and optical properties of monomers and their corresponding polymers. For this purpose, three different carbazole derivatives as a donor unit and thieno pyrrole dione and pyrrolo pyrrole dione as an acceptor units were choosen. Furthermore, to investigate the effect of alkyl substituent on the nitrogen atom, carbazole derivatives were chosen with and without alkyl chain.

3.2. Properties of the Monomers

3.2.1. Properties of M1

3.2.1.1. Electrochemical Properties of the M1

The electrochemical properties of **M1** were investigated in 0.2 M $TBABF_4$ / dry DCM electrolyte solution utilizing cyclic voltammetry and differential pulse voltammetry techniques. During the first anodic scan two reversible oxidation peaks at 1.17 V vs. Ag/AgCl and 1.48 V vs. Ag/AgCl were observed in the cyclic voltammogram CV of **M1** as depicted in Figure 3.1.a. However,

no reduction peak was noted during the cathodic scan. Differential pulse voltammogram (DPV) recorded in the same electrolytic solution also exhibited same reversible oxidation peaks (Figure 3. 1. b) confirming reversible electrochemical oxidation of **M1** in two consecutive electrochemical steps.

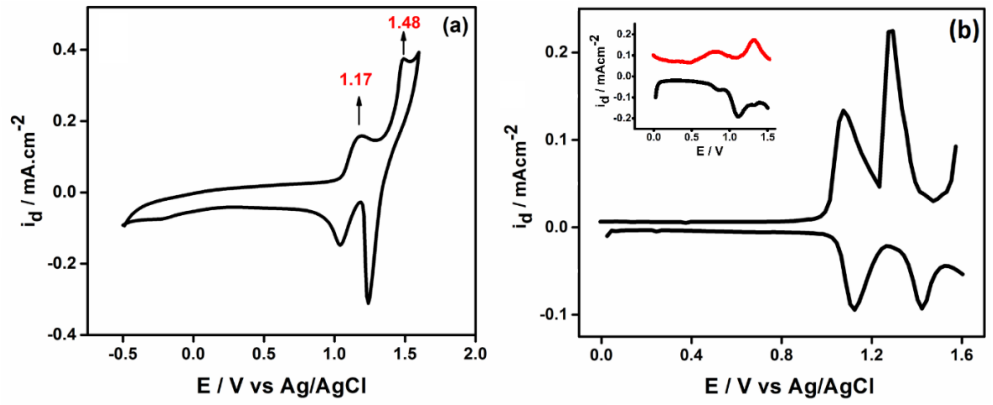


Figure 3. 1. CV **(a)** and DPV **(b)** of **M1** in 0.2 M $TBABF_4$/DCM electrolytic solution. Inset: DPV of **A1**

3.2.1.2. Optical Properties of M1

Electronic absorption spectrum of **M1** in DCM shows two absorption bands at 361 and 397 nm (Figure 3.2) due to π-π* and intramolecular charge transfer, respectively. Moreover, the monomer solution exhibits yellow color under day light and fluorescent yellow color under UV light. Fluorescence emission spectrum of **M1** recorded in DCM is also given in Figure 3.2. As seen from the figure there exit one strong emission band centered at 468 nm in the emission spectrum of **M1** corresponding to blue color. Comparison of absorption and emission maxima of the monomer solution reveals 71 nm Stokes shift indicating the conformational changes of the molecules upon excitation.[64]

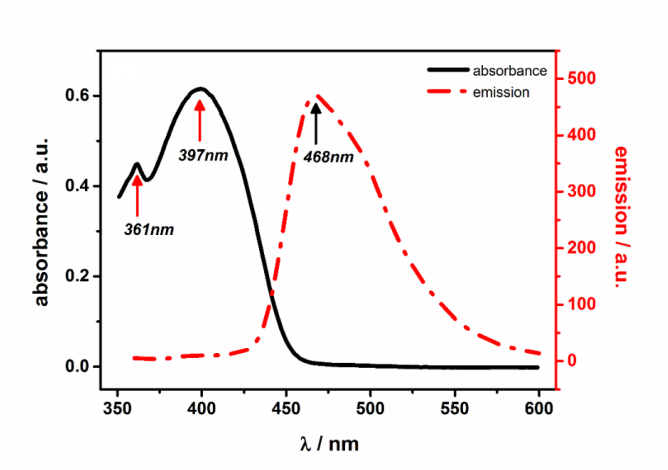


Figure 3. 2. Uv-Vis spectrum (solid line) and fluorescence spectrum (dash line) of **M1** in DCM (excited at 350 nm).

3.2.2. Properties of M2, M3 and M4

3.2.2.1. Electrochemical Properties of the M2, M3 and M4

To observe electrochemical properties of the monomers, their CVs and DPVs were recorded in dry DCM containing 0.2 M $TBAPF_6$ as supporting electrolyte and the results were given in Figure 3. The DPV of **M2** revealed two reversible and one irreversible oxidation peaks at 0.67 V, 0.92 V and 1.65 V vs. Ag/AgCl, respectively (Figure 3.3. a). Similar electrochemical behavior was observed for **M3**, two reversible and one irreversible oxidation peaks at 0.69 V, 0.92 V and 1.65 V vs. Ag/AgCl (Figure 3.3. b). Comparison of these values clearly indicates that substituent on the nitrogen atom (i.e. methyl and ethyl) of C-3 linked carbazoles does not influence the oxidation/reduction potentials of the monomers. In the case of **M4**, in which donor unit linked to the acceptor via C-2 position, two reversible oxidation peaks slightly shifted to more positive potentials as compared to **M2** and **M3** (first reversible oxidation peak ($E_{ox,1}$)= 0.75 V and second reversible oxidation peak ($E_{ox,2}$)= 1.01 V vs. Ag/AgCl). The irreversible peak on the other hand shifted to lower potential ($E_{ox,3}$ =1.36 V vs.

Ag/AgCl) (Figure 3.3.c). This relatively large cathodic shift in the irreversible oxidation peak might be due to the effect of different linkage site. It is known that in donor-acceptor type monomers containing 2-7 linked carbazoles exhibited higher conjugation as compared to 3-6-linked derivatives. The reversible reduction peak, on the other hand, appeared almost at the same potential as that of **M2**. This is expected, since all three monomers have the same acceptor group. To get more insight on the redox behaviour of the monomers we have also recorded DPV of the acceptor unit (**A2**) in the same electroltic medium and the resulting voltammogram is given in Figure 3.4. As seen from the Figure 3. 4 **A2** exhibits two reversible oxidation and one reversible reduction peaks similar to that of the monomers. On the other, no irreversible oxidation peak was observed in the potential range of 0.0 to 1.80 V. All the electrochemical data obtained from DPV measurements under the same conditions were also tabulated in Table 3.1 for comparison reason. A close inspection of Table 3.1 reveals that the reduction potentials of the three monomers are almost the same as that of **A2** because the reduction potential is determined by LUMO energy levels of the molecules. However, the two reversible oxidation peaks, originating from the acceptor part of the monomers, are shifted to lower potentials due to electron donating ability of carbazole units which increase the HOMO level. This shift is more pronounced for **M2** and **M3** because of higher electron donating strength of 3,6 carbazole as compared to 2,7-carbazole.[65]

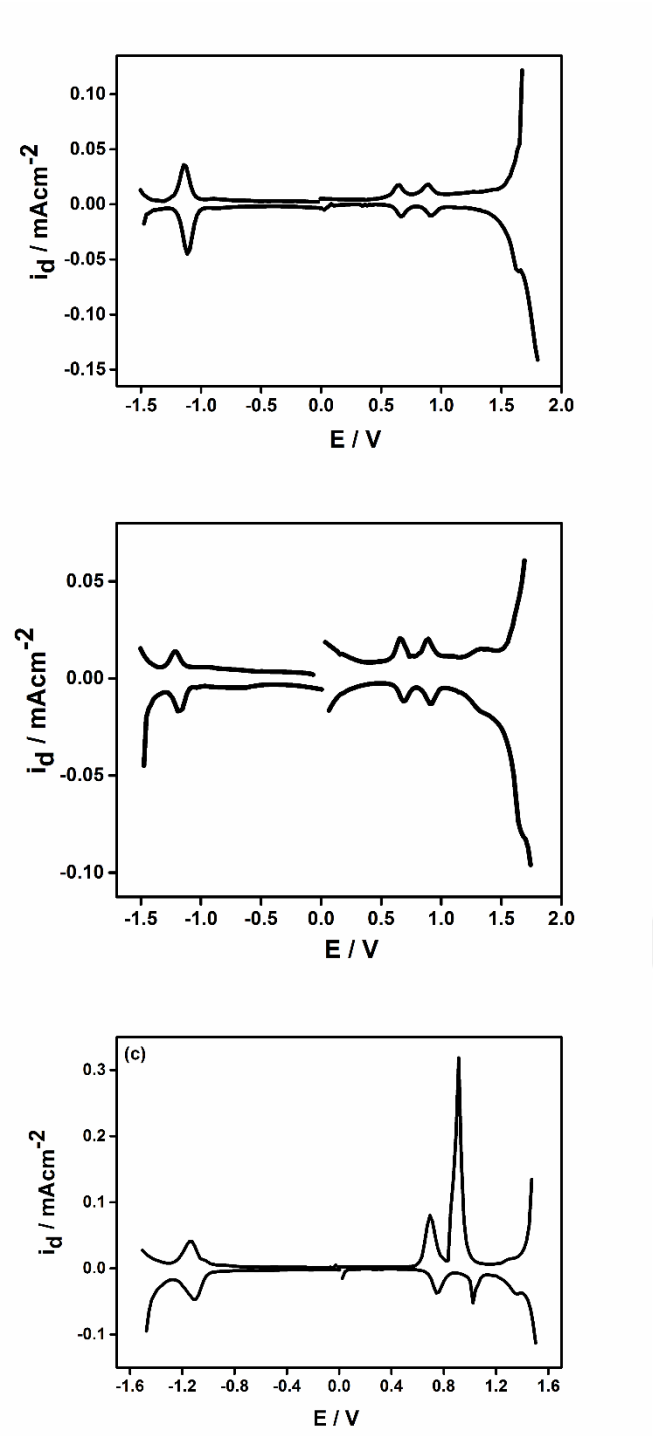


Figure 3. 3. DPV of **(a) M2** (**b**) **M3** and (**c**) **M4** in 0.2 M $TBAPF_6$/DCM electrolytic solution. (Step Size 20 mV sample period, 1 s, pulse time 0.1 s and pulse size 25mV).

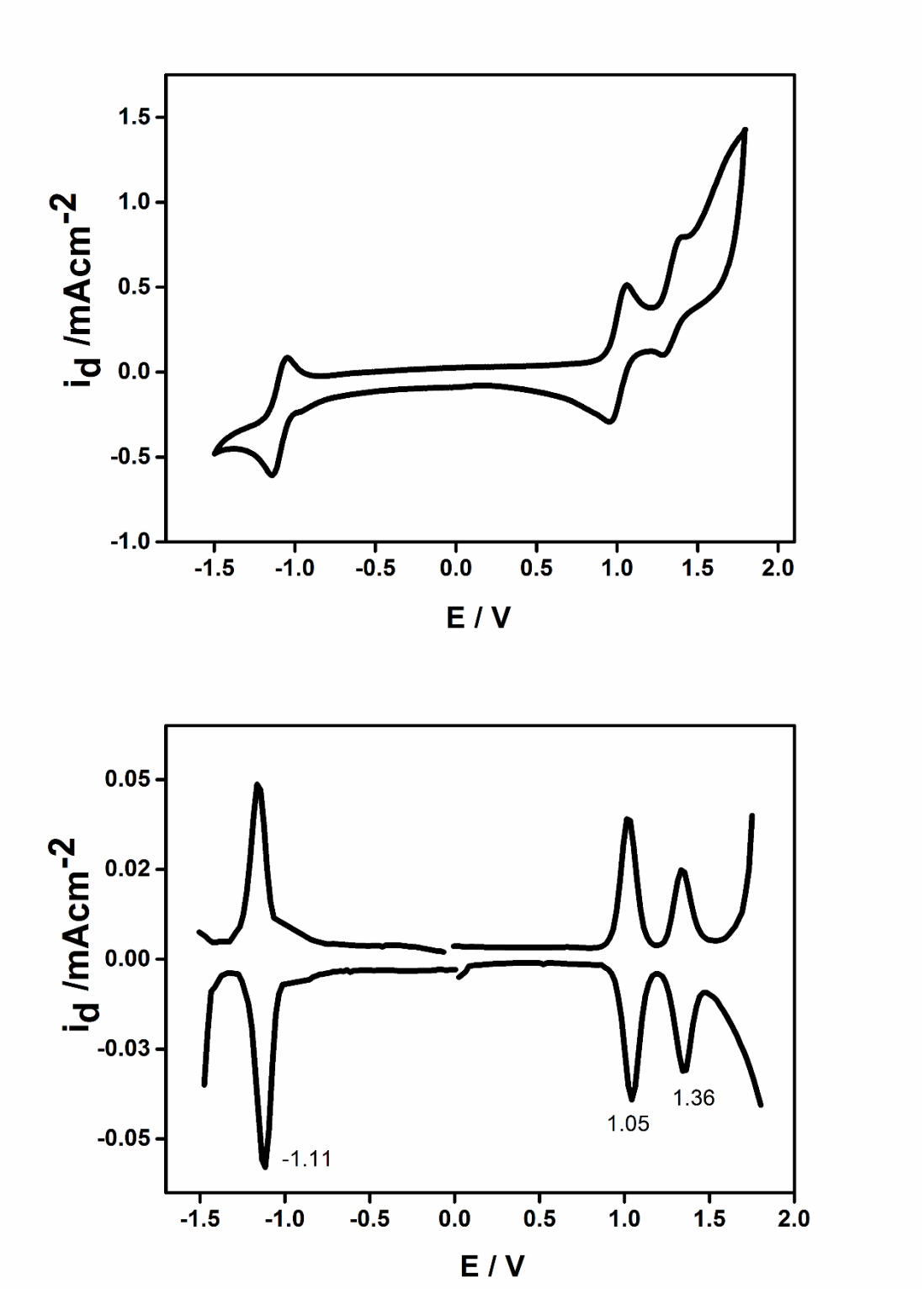
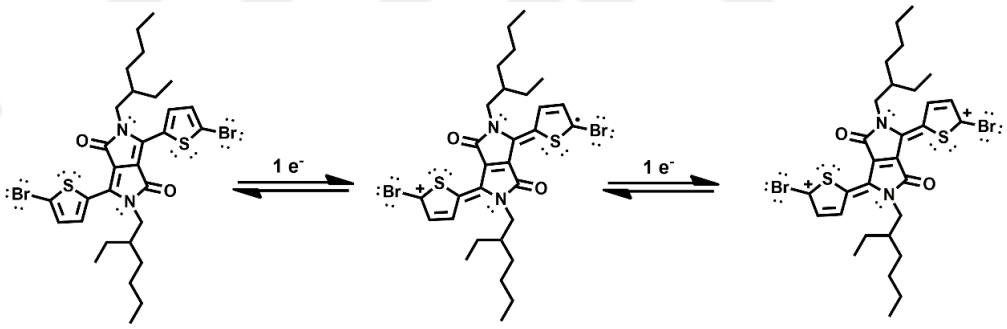


Figure 3. 4. **(a)** CV and **(b)** DPV of **A2** in 0.2 M $TBAPF_6$/DCM electrolytic solution (Step Size 20 mV sample period, 1 s, pulse time 0.1 s and pulse size 25mV for DPV).

Table 3. 1. Electrochemical data of monomers and **A2** vs. Ag/ AgCl.

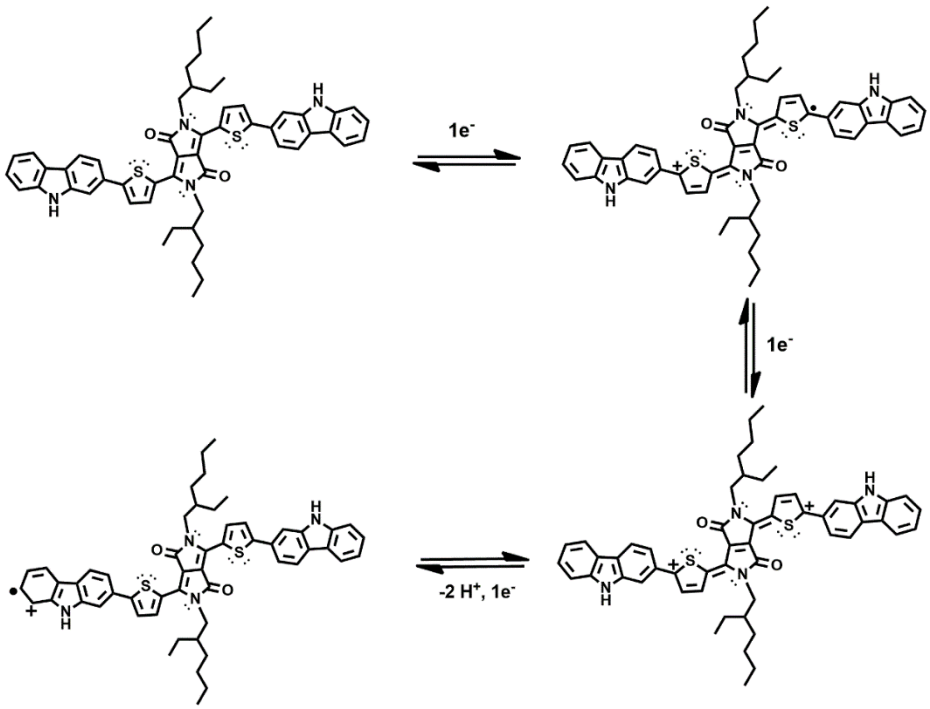
Monomer	$E_{ox,1}$ (V)	$E_{ox,2}$ (V)	$E_{ox,3}$ (V)	E_{red} (V)
M1	1.17	1.48	-	-
M2	0.67	0.92	1.63	-1.13
M3	0.69	0.92	1.65	-1.21
M4	0.75	1.01	1.36	-1.12
A2	1.05	1.36	-	-1.15

In the light of the experimental data obtained from DPV, the following reaction mechanism for the two steps reversible oxidation of **A2**, can be suggested (Scheme 3.1), which is consistent with previously reported mechanism for diketopyrrolopyrrole central accepting unit symmetrically disubstituted with bithiophene . [66]

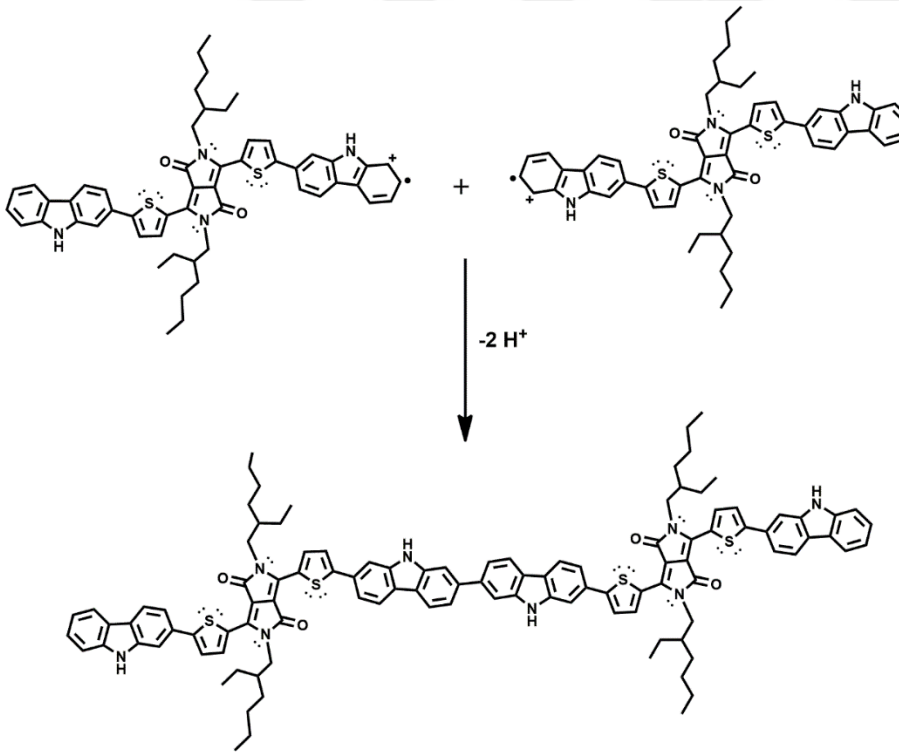


Scheme 3. 1. Two steps reversible oxidation of A2.

A similar mechanism for three step electrochemical oxidation of **M4** and its radical coupling reaction mechanism are given in Scheme 3.2 and 3.3, respectively.



Scheme 3. 2. Suggested mechanism for three step oxidation of **M4**



Scheme 3. 3. Radical coupling step of electro-oxidative polymerization for **M4**

3.2.2.2. Optical Properties of M2, M3 and M4

The optical properties of monomers, **M2, M3** and **M4** were investigated by recording their electronic absorption spectra in DCM and results are shown in Figure 3.5. Inspection of Figure 3.5 reveals that the monomers exhibit similar absorption features irrespective of linkage site and substituent on the nitrogen atom. In the case of **M2**, there exist two bands in the UV region of spectrum, at 328 and 415 nm, and a stronger band with vibronic feature at about 600 nm. The vibronic structure of the shorter wavelength band is typical for DPP dyes[67] and can be attributed to intramolecular charge transfer (ICT). The band that appears at 415 nm is attributed to π-π* transition. Replacement of methyl substituent on the N-atom in **M2** with ethyl substituent, **M3**, results in a 10 nm red shift. This small bathochromic shift indicates relatively stronger ICT in **M3** as compared to **M2**. In the case of **M4**, in which the donor unit linked to acceptor unit via C-2 position, both π-π* transition and ICT bands exhibit small hypsochromic shift indicating weaker ICT in **M4** as compared to **M2** and **M3**. The fluorescence emission spectra of all the monomers, recorded in DCM, exhibited strong luminescence maxima at about 650 nm upon their excitation at 550 nm. Mirror images are obtained for the absorption and emission spectra which suggest a similar geometry in the ground and first excited state.[65] In order to confirm that longer wavelength bands in the electronic absorption spectrum of monomers are due to ICT, fluorescence emission spectrum of **M3** was also recorded in the solvents having different polarities and the results are depicted in Figure 3.6. As seen from the figure, the emission maximum red shifts with increasing solvent polarity ($\lambda_{emission}$= 649 nm (toluene, $\varepsilon = 2.38$), 652 nm (DCM, $\varepsilon = 8.93$) and 663 nm (dimethylsulfoxide (DMSO, $\varepsilon = 46.7$) clearly indicating that the longer wavelength band in the electronic absorption spectra of the monomers are due to ICT.

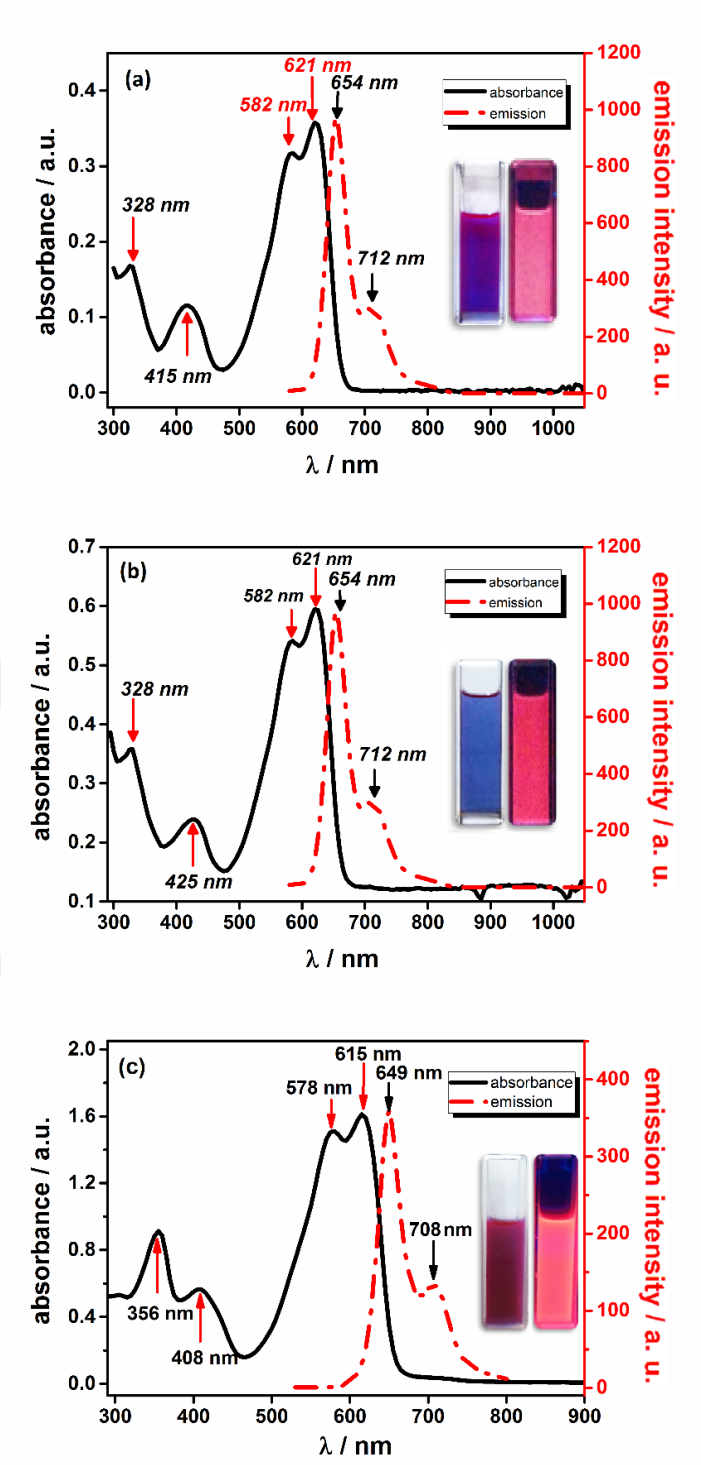


Figure 3. 5. Uv-Vis spectra and PL spectra of (**a**) **M2,** (**b**) **M3** and (**c**) **M4** in DCM. Inset of (**a**), (**b**) and **(c)** are photographs of **M2**, **M3** and **M4** were taken under day light and UV lamp. (Excitation at 550 nm)

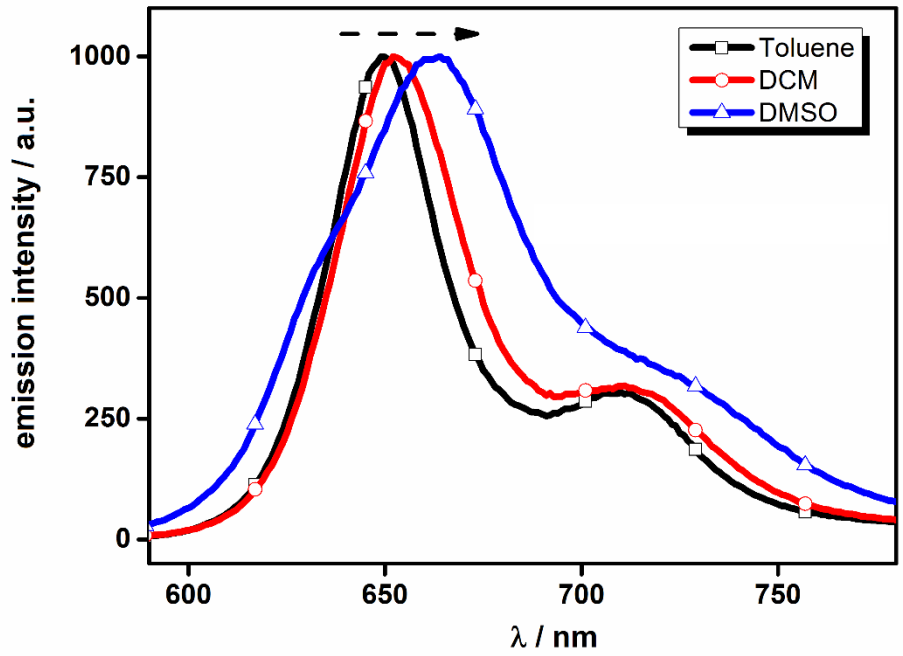


Figure 3. 6. Fluorescence emission spectra of **M3** in toluene, DCM and DMSO (Excitation at 550 nm)

3.3. Electrochemical Polymerization and Characteristics of the Polymers

3.3.1. Electrochemical Polymerization of M1

After electrochemical and optical characterization of the monomer M1 was completed, its electrochemical polymerization was studied via potentiodynamic and potentiostatic methods in DCM-$TBABF_4$ electrolytic medium. However, no sign of polymerization was observed when the potential was cycled repetitively between 0.0 and +1.20 V (first oxidation potential of the monomer). When the scan limit was extended to + 1.50 V (slightly greater than the second oxidation peak) small amount of deposition on the electrode surface was observed but due to its low adherence on the surface, no polymer film was obtained on the working electrode surface. In the case of

potentiostatic attempt, a small quantity of boron trifluoride diethyl etherate (BFEE) (60 μL to 3.0 mL electrolytic solution) was added not only to resolve the adherence problem and also to lower the oxidation potential of monomer by lowering aromatization energy. Then, the potential was set to 1.30 V which resulted formation of a very thin film on the surface of the working electrode.

3.3.2. Optical and Electrochemical Characteristics of the PM1

Spectroelectrochemical studies were performed in order to elucidate opical and electrochemical properties of the polymer film, **PM1**. As explained above (part 3.3.1) a very thin polymer film was deposited on ITO electrode at +1.3 V in DCM-$TBABF_4$ electrolytic medium containing 60.0 μL BFEE. **PM1** coated ITO electrode was transfer into solvent free electrolytic solution and the changes in the electronic absorption spectrum of **PM1** film was monitored as a function of WE potential and the results are given in Figure 3.7. As seen from the Figure 3.7, the π-π* transition band at 391 nm slightly losses intensity which is accompanied by the formation of a weak broad band beyond 800 nm during the potential scan from 0.0 to +1.2 V at a voltage scan rate of 20 mV/s. These slight changes, due to poor quality of **PM1** film, are also accompanied with color change from yellow to light brown (see inset of Figure 3.7.b). The CV recorded during in-situ spectroelectrochemical studies was also given in Figure 3.8. As seen from the figure, **PM1** exhibits reversible redox couple (E_{ox}=0.84 V and E_{red}= 0.65 V) due to doping and de-doping of polymer film.

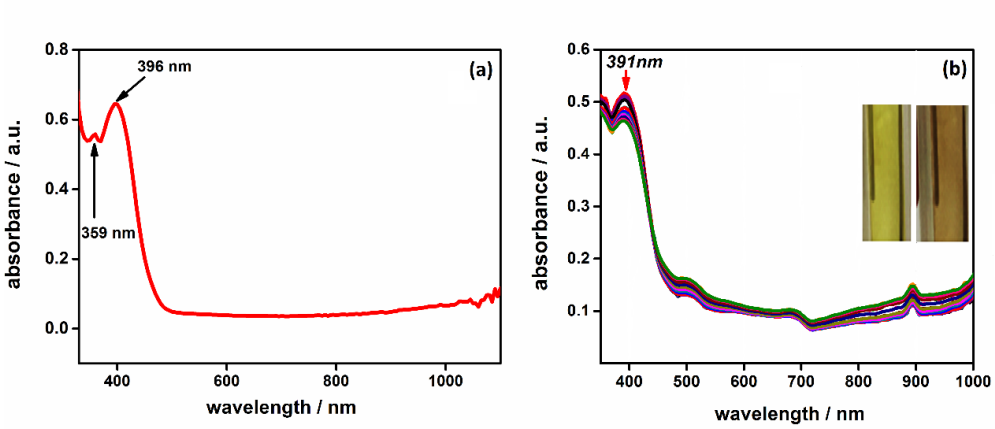


Figure 3. 7. (a) Absorbance spectrum of **PM1** in ACN on ITO coated glass and **(b)** spectroelectrochemistry of **PM1** film on an ITO coated glass in a monomer free 0.1 M ACN-$TBABF_4$ solution at applied potential range which is between -0.5 V and 1.2 V.

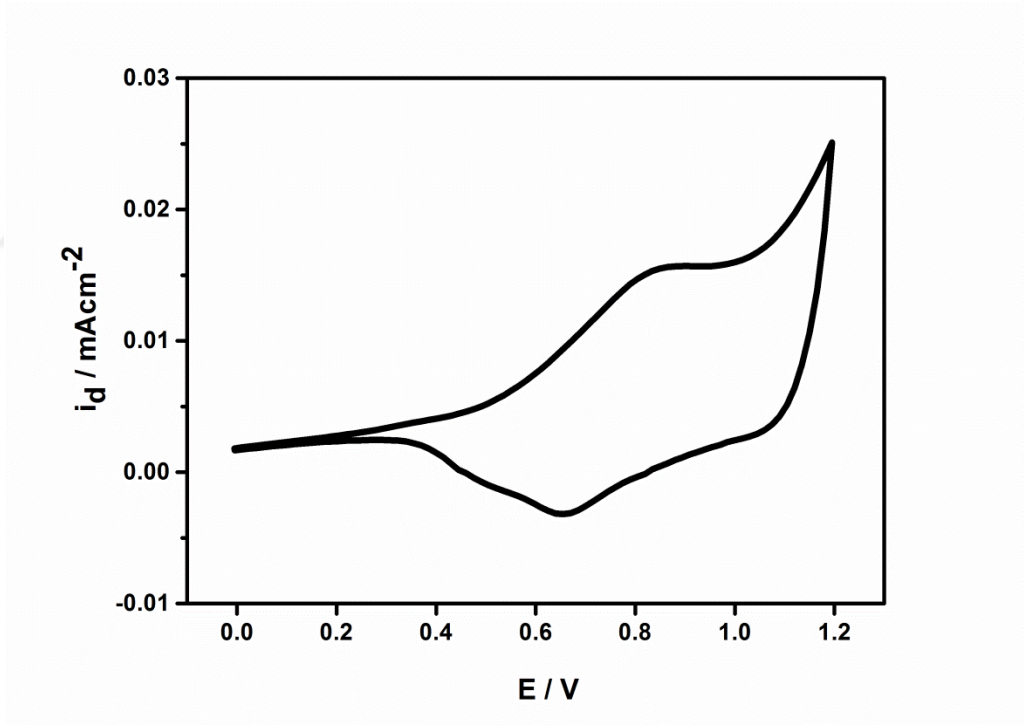


Figure 3. 8. CV of **PM1** in 0.1 M ACN-$TBABF_4$ monomer free solution on ITO glass working electrode, at a scan rate of 20 mV.s^{-1}.

Optical band gap (E_g) value of the polymer film in their neutralstate wasalso calculated from the onset of the low energy end of π-π* transition band and was found to be 2.70 eV. HOMO/LUMO energy levels of the polymer was elucidated utilizing their ionization potentials and electron affinities obtained from experimental data. The onset of oxidation potentials of **PM1** (0.54 V) was used as E_{ox} in the following empirical equation.[68]

$I_p = -(4.8 + E_{ox}) = -5.34$ eV

Electron affinity was estimated by subtracting the band gap energy from I_p and was found to be -2.64 eV.

3.3.4. Copolymerization of M1 with EDOT

3.3.4.1. Electrochemical Copolymerization of M1 with EDOT

Due to high band gap and low adherence of **M1** we have investigated its copolymerization with EDOT. Copolymers of EDOT and **M1** were prepared using different monomer feed ratios by repetitive potential cycling in order to investigate its effect on band gap tuning.

Prior to copolymerization studies DPV of **M1** and EDOT were recorded in DCM-TBABF4 electrolytic medium and the results are given in Figure 3.9. As seen from the Figure 3. 9, the oxidation potentials of **M1** and EDOT are compatible to obtain a copolymer via electrochemical techniques.

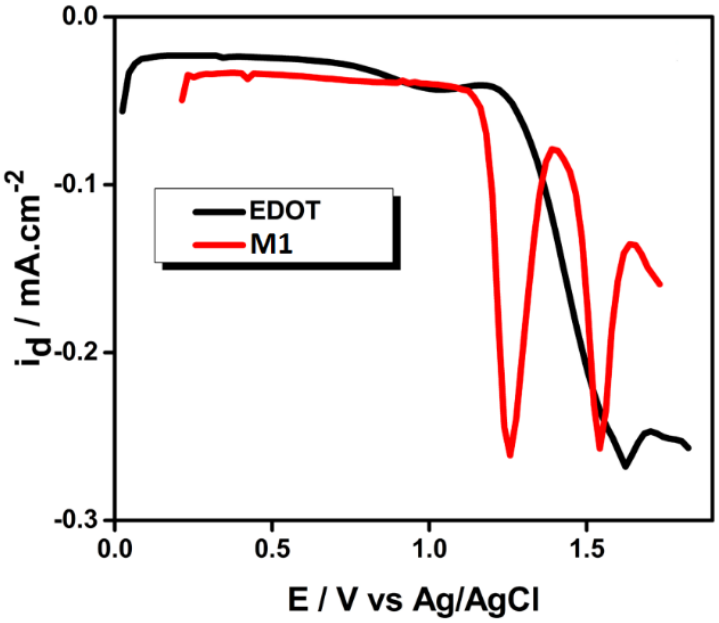


Figure 3. 9. DPVs of **M1** and EDOT during their anodic scans in 0.1 M DCM-$TBABF_4$.

Copolymers were prepared utilizing CV technique by applying 20 repetitive cycles between a certain potential range of -0.8 V and 1.5 V in an electrolytic solution of 0.1 M DCM-$TBABF_4$ (Figure 3.10). As seen from the Figure 3.1 (a-b-c-d), after the first anodic scan a new redox couple starts to intensify upon successive cycling in the case of EDOT and co-monomer mixtures with different feed ratios which indicate polymer deposition on the working electrode surface. When the second and last cycles recorded during electropolymerizations were compared (Figure 3.10. e and 3.10. f, respectively) a decrease in the current densities were noted with increasing **M1**/EDOT ratio (i.e. from 1:9 to 1:1) due to decreasing electroactivity of copolymer as compared to PEDOT. The characteristic anodic and cathodic peaks (1.2 V and 1.0 V, respectively) of **M1** becomes clearly noticeable in the co-monomer mixture and their intensities increase with increasing **M1**/EDOT ratio (Figure 3-10e). Appearance of these characteristic anodic-cathodic peaks of **M1** in the CVs of polymer films indicates incorporation of **M1** into the polymer matrix. The decrease in the current density with increasing the **M1** in

the monomer feed ratio further proves the copolymer formation during repetitive potential cycling.[69] After completion of electropolymerization (20 repetitive cycles) monomeric or oligomeric parts were removed by washing the polymer films with DCM and the CVs of PEDOT and copolymer films were recorded in monomer free solution between -1.0 V and 1.0 V (Figure 3. 10. g). Although current density decreases with decreasing EDOT in the feed ratio, characteristic capacitive behavior of PEDOT was still observable in the copolymer films.

It is important to note that, when the monomer feed ratio reaches to 1, the problem observed during homopolymerization of **M1** was also noted; causing loss of some part of polymer film from the electrode surface into the electrolytic solution. However, the remaining polymer film on the surface was still enough to reflect a different behavior from PEDOT (See Figure 3. 10. f and 3. 10. g).

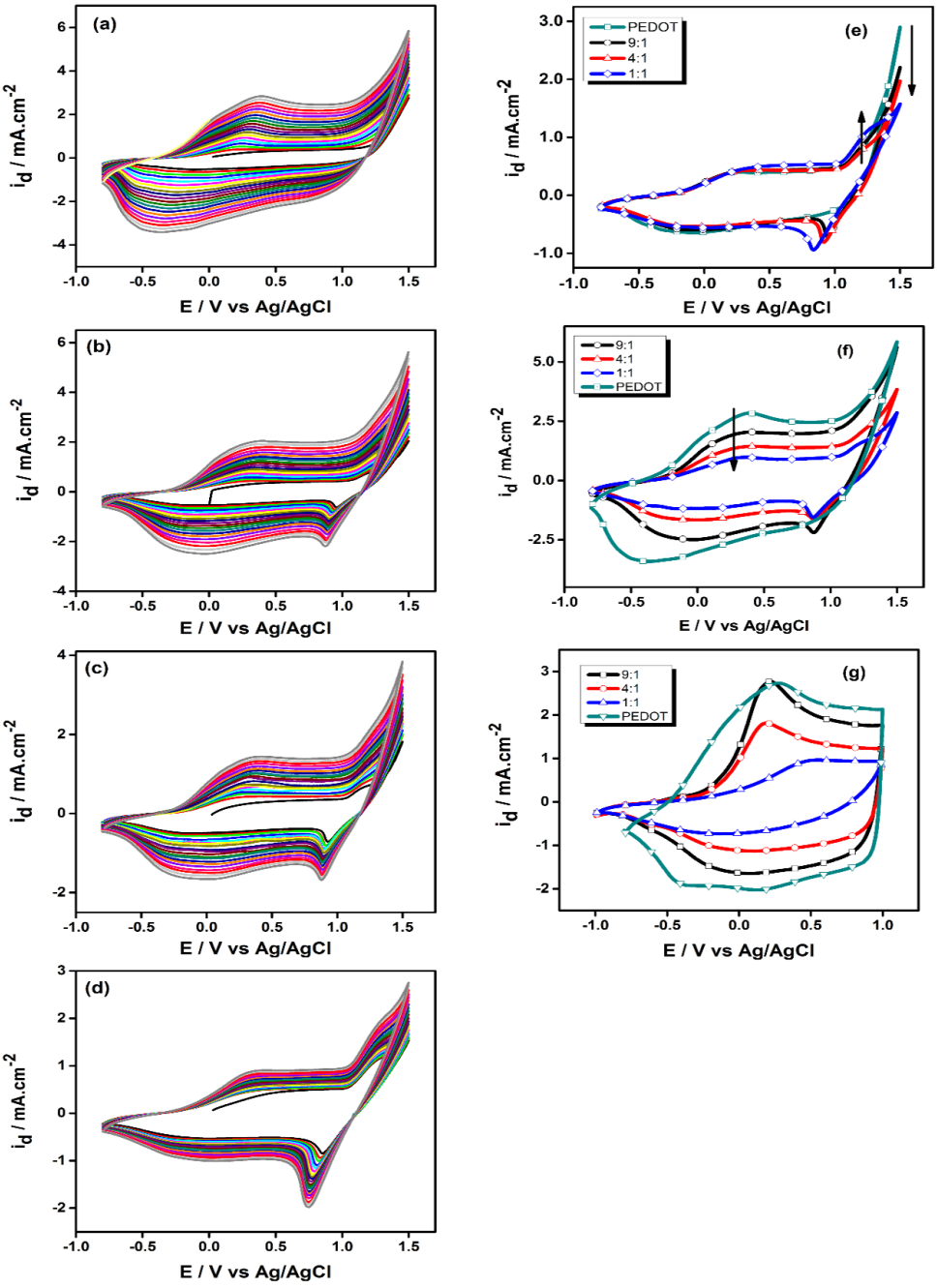


Figure 3. 10. CVs of EDOT **(a)** and EDOT/**M1** monomer feed ratios of 9:1 **(b)**; 4:1 **(c)** and 1:1 **(d)** during electropolymerization on Pt WE between -0.8 V and 1.5 V in 0.1 M DCM-$TBABF_4$ with a scan rate of 100 $mV.s^{-1}$. The second **(e)** and the last **(f)** CVs of the electropolymerization cycles. **(g)** CVs of PEDOT and resulting copolymers in a monomer free solution containing 0.1 M $TBABF_4$ in ACN.

The copolymer films were scanned with increasing scan rates between -1.0 V and 1.0 V in order to observe their scan rate dependency. The copolymers exhibited a linear increase in current densities with increasing scan rates indicating well adhering electro-active polymer film on the electrode surface and the non-diffusional redox behavior even at high scan rates.[70] The scan rate dependence of the copolymer (4:1) was demonstrated in Figure 3.11 as a representative example.

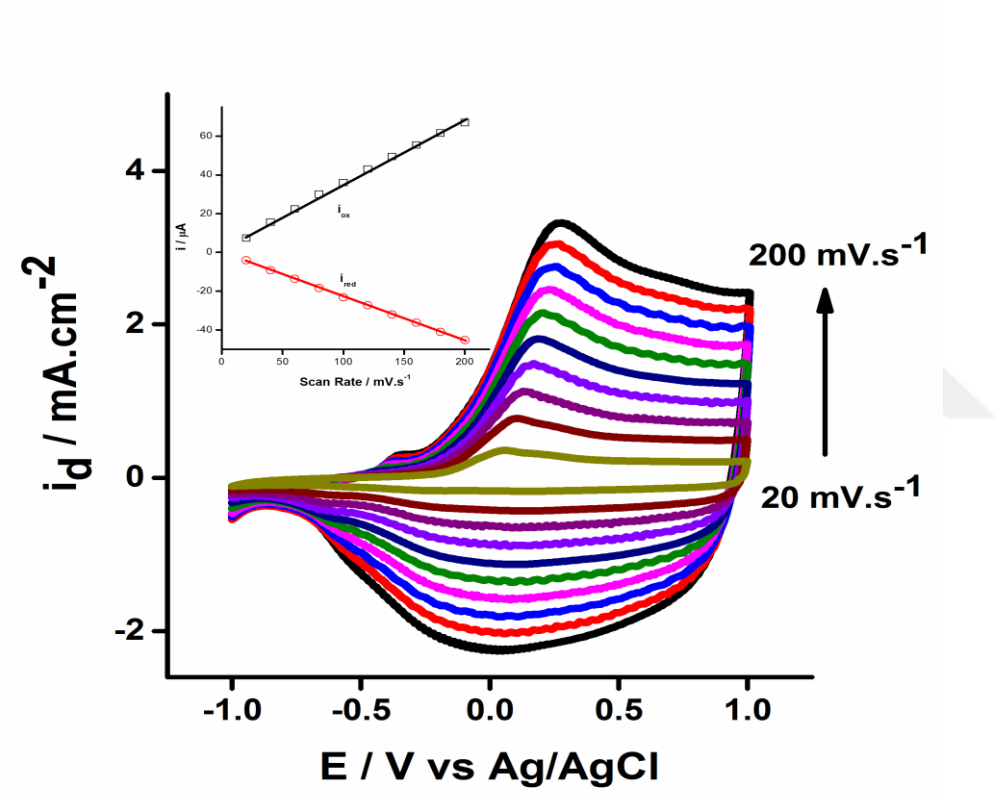


Figure 3. 11. The CVs of the copolymer (4:1) with increasing scan rate from 20 mV.s^{-1} to 200 mV.s^{-1} with 20 mV increments. (0.1 M DCM-TBABF$_4$ monomer free solution, on Pt working electrode vs Ag/AgCl). Inset: Variation of anodic and cathodic current densities vs voltage scan rate.

3.3.4.2. Spectrochemical properties of the copolymers

The copolymer films were also investigated in terms of their optical behaviors which were obtained on ITO working electrode surface via constant potential electrolysis by applying 1.5 V potential until the same amount of charge of 50 $mC.cm^{-2}$ passed through the system. For comparison sake EDOT and **M1** homopolymers (PEDOT and **PM1**) were also prepared on the ITO working electrode surface. After washing with DCM, polymer film coated electrodes were dipped into monomer free electrolytic solution and were brought into their neutral form by applying -1.0 V potential for 60 s. Electronic absorption spectra of homo and copolymers are given in Figure 3.12. As seen from the figure, all copolymer films exhibit a strong absorption band having maximum at around 595 nm originating from PEDOT unit. However, in the case of copolymer films, apart from 595 nm band, there exists another band at about 410 nm which is originating from **M1**. It is noteworthy to mention that the intensity of this shorter wavelength band increases with increasing **M1**/EDOT ratio in the electrolytic solutions clearly indicating incorporation of **M1** units into the copolymer structure.

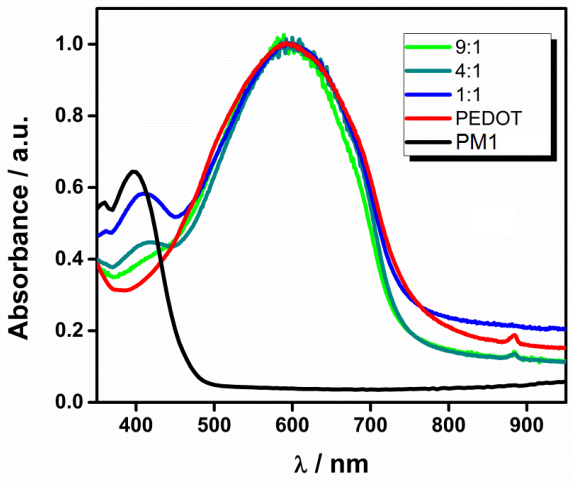


Figure 3. 12. Normalized electronic absorption spectra of the copolymer and homopolymer films in their neutral forms recorded in ACN.

Electro-optical properties of the copolymer films deposited on ITO electrode via constant potential electrolysis were also investigated by monitoring the changes in the electronic absorption spectra under a voltage pulse and the results are depicted in Figure 3.13.

As seen from the figure, both 410 nm and 595 nm bands lose their intensities during oxidation of the copolymer films which is accompanied by the appearance of new intensifying band located at 850 nm due to formation of charge carriers (i.e. polarons). Upon further oxidation, another band beyond 1000 nm was also noted indicating the bipolaron formation. These changes in the electronic absorption spectra were also accompanied by a color change blue to transparent blue for PEDOT,[71] yellow to deep yellow for **PM1** and blue to transparent green for the copolymer films in their neutral and oxidized states, respectively. The different colors of PEDOT (transparent blue) and copolymer films (transparent green) in their oxidized states can be explained in terms of differences in their electronic absorption spectra. A close inspection of Figure 3.13-e reveals that the copolymer films absorb visible light in two regions, a band around 410 nm and another one beyond 700 nm, which are essential values for the appearance of green color.[72] Moreover, a grayish color was observed in semi-oxidized states of copolymers which were not observed during oxidation of the homopolymers (Figure 3.13-f).

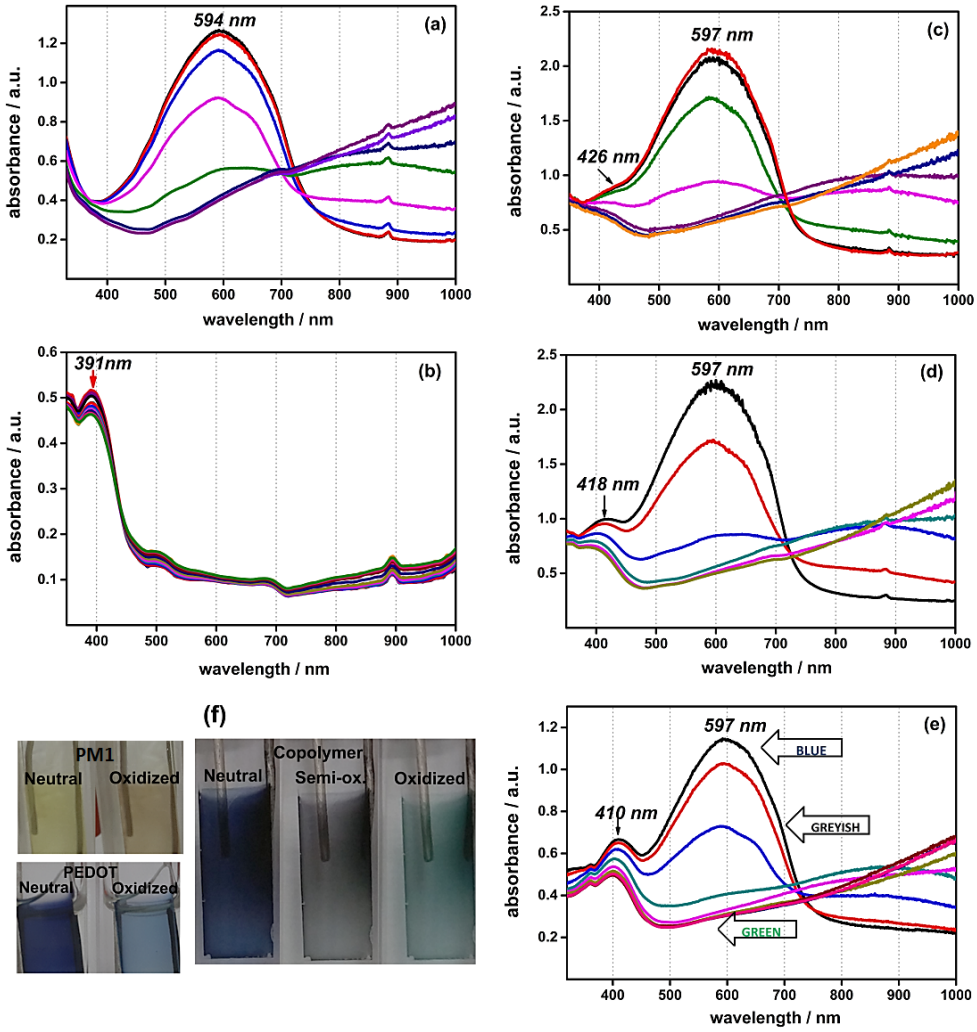


Figure 3. 13. Collected electronic absorption spectra of PEDOT **(a)**; **M1, (b)**; copolymers of 9:1, 4:1, 1:1 **(c, d, e**, respectively) during potential scanning from -1.0 V to 1.0 V in 0.1 M ACN-$TBABF_4$ monomer free solution with scan rate of 20 $mV.s^{-1}$ and colors of homopolymers and copolymer (4:1) in their neutral and oxidized states **(f)**. (For **PM1**, potential scanning range is between -0.5 V and 1.2 V).

CVs recorded during in-situ spectroelectrochemical studies were also given in Figure 3.12. As seen from the figure, the intensity in current decreases by the increasing amount of **M1** in monomer feed ratio. Moreover, onset oxidation

potentials of copolymer films approach to that of **M1** homopolymer (0.51 V) with increasing concentration of **M1** in the electrolytic solution.

Optical band gap values (E_g) of the copolymers and homopolymers were calculated from the onsets of π - π* transition bands in their neutral absorption spectra and the results were depicted in Table 1. The band gap energies of the copolymers did not show appreciable difference from that of PEDOT albeit they became much lower when compared to band gap of **M1** homopolymer (See Table 3.2).

Table 3. 2. Electrochemical and optical properties of the copolymer films and homopolymer films.

Copolymers (EDOT: **M1**)	E_{ox}^{onset} (V)	Absorption λ_{max} (nm)	E_g^{opt} (eV)
P(9:1)	-0.32	426 -590	1.67
P(4:1)	-0.42	418 - 597	1.67
P(1:1)	-0.35	410 - 594	1.66
PEDOT	-0.45	594	1.64
PM1	0.51	391	2.64

The percent transmittance values (%T) of the copolymer films at their low lying energy bands were calculated as % 27, %32 and 43 % for P(9:1), P(4:1) and P(1:1), respectively and % T of the PEDOT film was calculated as %35. As seen from the transmittance data, the copolymer formation results with higher T % values with increasing **M1** ratio in the co-monomer mixture.[70] However, the inverse trend was observed for their high energy bands. At their high energy bands, the transmittance percents were found as %15, %14 and %11 for P(9:1), P(4:1) and P(1:1), respectively, further indicating the increasing amount of **M1** contribution in the copolymers.

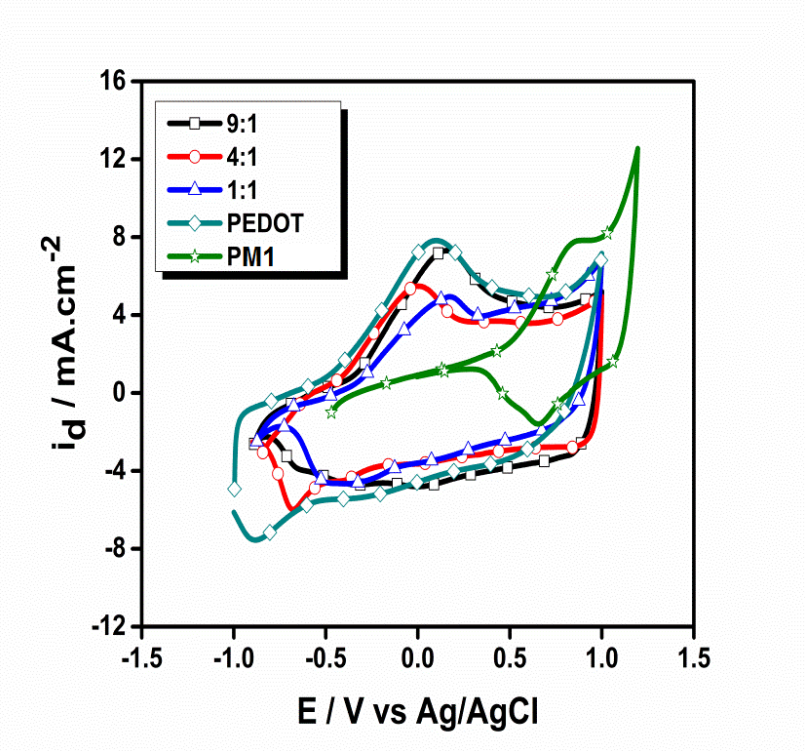


Figure 3. 14. CVs of copolymer and homopolymer films on ITO WE, recorded in 0.1 M ACN-$TBABF_4$ monomer free solution with scan rate of 20 $mV.s^{-1}$

3.3.5. Electrochemical Polymerization of M2, M3 and M4

After the determination of redox behaviors of the monomers (**M2**, **M3** and **M4**), repetitive anodic scans were performed to get their corresponding polymers **PM2**, **PM3** and **PM4**. Since the monomers which are synthesized in this work have relatively higher oxidation potentials which might adversely affect the properties of obtained polymers, we tried to lower the oxidation potential necessary to initiate the polymerization, namely, third irreversible oxidation potential of the monomers. It is known that in the presence of BFEE the oxidation potentials of heteroaromatic systems are lowered due to lowering aromatization energy.[73] Therefore, to see the effect of BFEE on our monomers, we recorded also their DPVs in the presence of BFEE. For this purpose, 60 µL

BFEE was added into 2.00 mL electrolytic solution and the resulting voltammograms are given in Figure 3.15. As seen from the Figure 3. 15 $E_{ox,3}$ for the monomers shifted to lower potentials upon addition of BFEE to the electrolytic solution (from 1.65 V to 1.40 V for **M2**, from 1.65 V to 1.32 V for **M3** and from 1.36 V to 1.30 V for **M4**).

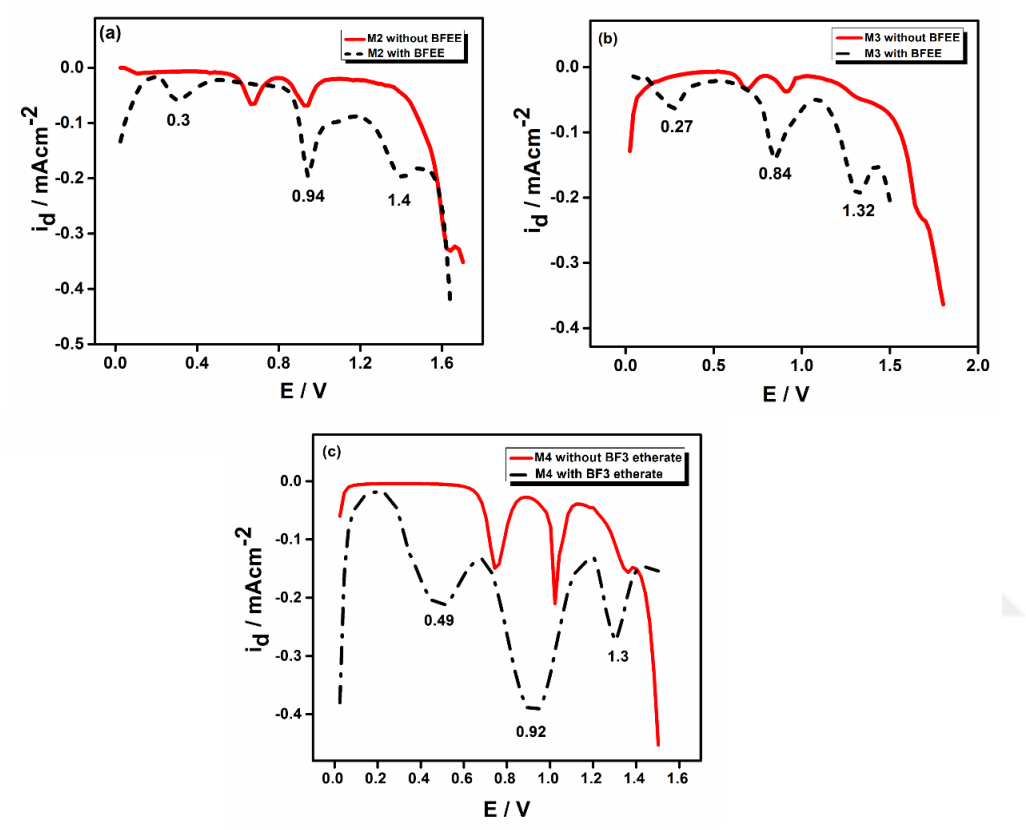


Figure 3. 15. DPV of **(a) M2**, **(b) M3** and **(c) M4** with and without BFEE (Step Size 20 mV sample period, 1 s, pulse time 0.1 s and pulse size 25mV).

Electrochemical synthesis of the polymers was performed in DCM containing 0.2 M $TBAPF_6$ as supporting electrolyte together with 60 μL BFEE. Pt-bead or ITO was used as working electrode. Electrochemically synthesized polymers were obtained with 50 cycles (200 mV/s) via repetitive cycling within the range 0.0-1.4 V for **M2**, **M3** and **M4**. As shown in Figure 3.16, during second anodic scan, new redox couples appeared around 0.8 V, indicating electroactive polymer film formation on the electrode surface. After each following cycle, the current increased steadily which indicated that both the surface area and the thickness of the polymer film on the WE also increased.

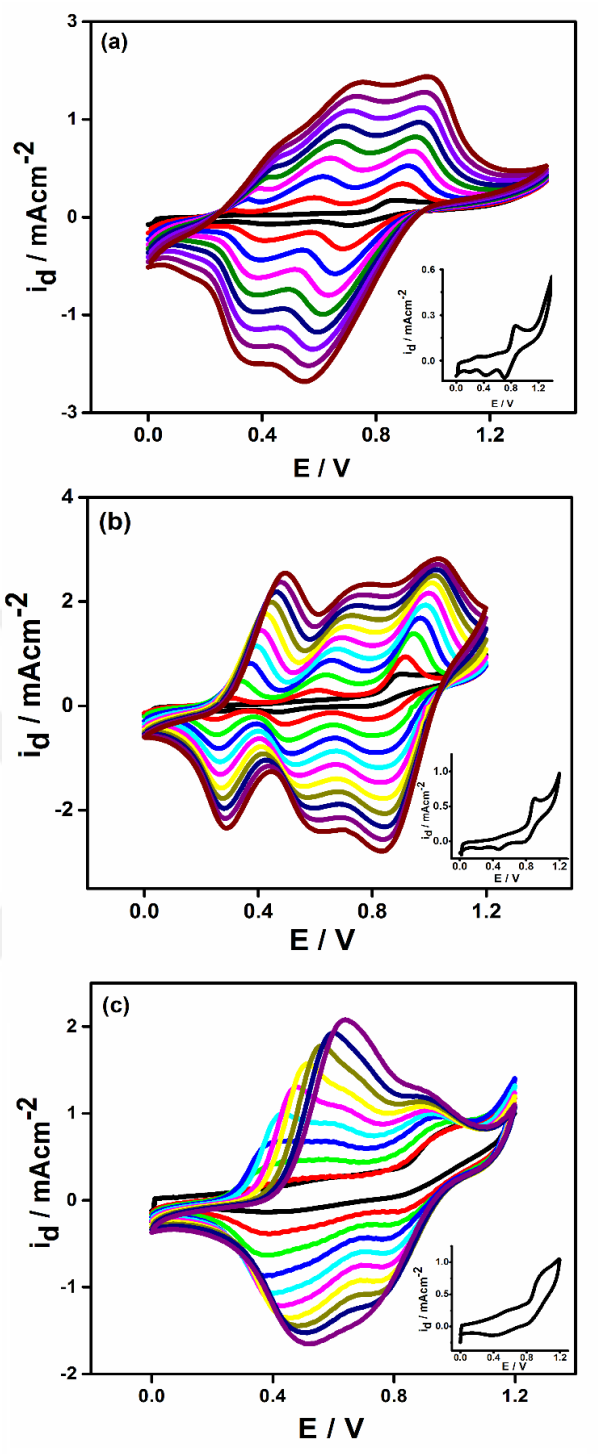


Figure 3. 16. Electropolymerization of the monomers **a) M2**, **b) M3**, and **c) M4** in 0.2 M $TBAPF_6$, BFEE: DCM (0.03:1- v:v) solution on a Pt disc electrode at 100 mVs^{-1} (50 cycle). Insets given in the figures represent the first cycles of CV.

3.3.6. Electrochemical Characteristics of the PM2, PM3 and PM4

After completion of the polymer formation, the polymer film coated on WE was washed with ACN to remove any unreacted monomer and oligomeric species. The electrochemical behavior of the polymer films were investigated by recording their CVs in a monomer free electrolytic solution consisting of 0.1 M $TBABF_4$ in ACN (Figure 3.17). All three polymer films exhibits two reversible oxidation and one reversible reduction peaks indicating the formation of charge carriers on the main chain due to doping and de-doping of the polymer films. In order to elucidate electrochemical band gap values, oxidation and reduction onset values were evaluated from the voltammograms of the polymer films and the results are given in Table 3.3 including calculated E_g^{el} values.

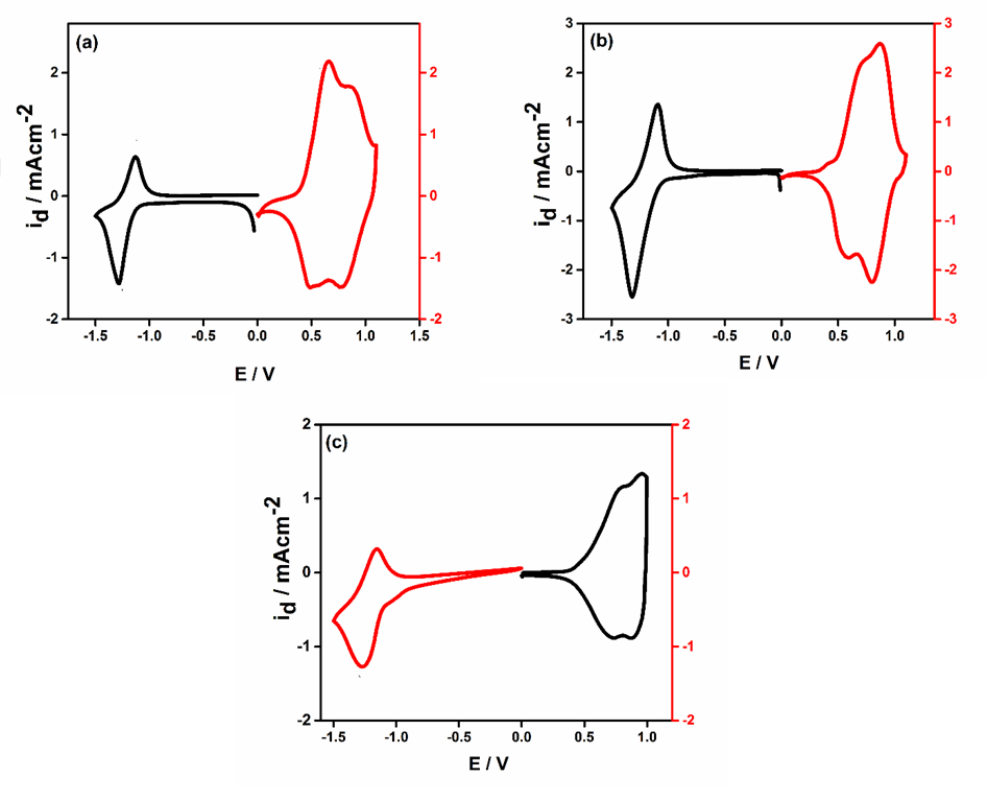


Figure 3. 17. Cyclic voltammograms of **(a) PM1**, **(b) PM2** and **(c) PM3** film in 0.1 M $TBABF_4$/ACN at scan rate of 200 mVs^{-1}

As shown in Table 3. 3 E_g^{el} values of the polymers show slight variations due to different electron donating ability and different steric hindrance of donor groups. Furthermore, HOMO/LUMO energy levels were also calculated for the polymer films utilizing the following equation.

E (HOMO, eV) = - (E_{ox}^{ons} + 4.80) where the energy level of Fc/Fc^+ was taken as 4.8 eV under vacuum.[67] LUMO energy levels were estimated by subtracting the band gap energy from the HOMO energy level and the results are tabulated in Table 3.3. The HOMO energy levels of the polymer film elucidated from electrochemical measurements were found to be in accordance with previously reported values for similar 2,7 -linked carbazole DPP polymers prepared by Suzuki coupling.[74,75]

Table 3. 3. Oxidation - reduction onsets and electronic band gap of **PM2**, **PM3** and **PM4** according to CV.

	E_{red}^{onset}	E_{ox}^{onset}	HOMO (eV)	LUMO (eV)	E_g^{elec}
PM2	-1.14	0.40	-5.20	-3.66	1.54
PM3	-1.05	0.43	-5.23	-3.74	1.49
PM4	-1.09	0.51	-5.31	-3.71	1.60

Furthermore, a linear increase in the peak currents as a function of the scan rates confirmed well-adhered electroactive polymer films on the electrode surface as well as non-diffusional redox process (Figure 3.18 and insets).

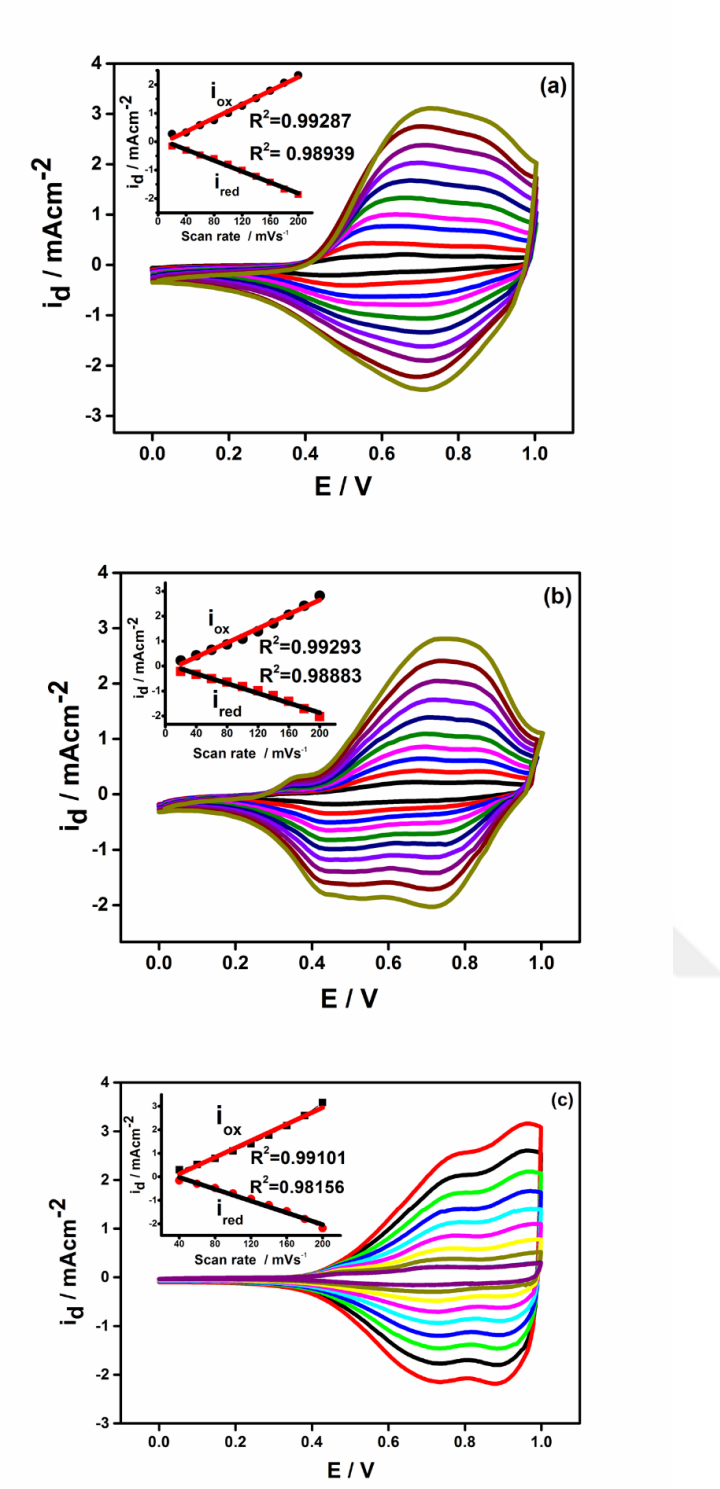


Figure 3. 18. Scan rate dependencies of electrochemically synthesized **(a) PM2**, **(b) PM3** and **(c) PM4** in 0.1 M $TBABF_4$/ACN at scan rates of 20-200 mV/s (Insets: Relationship of anodic and cathodic currents with respect to scan rate)

3.3.7. Spectroelectrochemical Properties of the Polymers

In order to elucidate the electrochromic features and to get information about charge carriers polymer films were deposited on ITO working electrode (30 $mC.cm^{-2}$) via constant potential electrolysis at 1.20 V. The changes in the electronic absorption spectrum were recorded during potential scanning from -0.5 V to 1.0 V for **PM2** and **PM3** from -0.5 V to 1.2 V for **PM4**, with a voltage scan rate of 10 mV/s, in a monomer free electrolytic solution, and the results are depicted in Figure 3.18. An inspection of figure reveals that all polymer films exhibit strong absorption bands at about 595 nm, 596 nm, and 584 nm for **PM2**, **PM3** and **PM4**, respectively (see Table 3. 4). Upon oxidation, these bands loose intensities, at the same time new bands are formed at 892 nm, 870 nm and 855 nm for **PM2**, **PM3** and **PM4**, respectively.

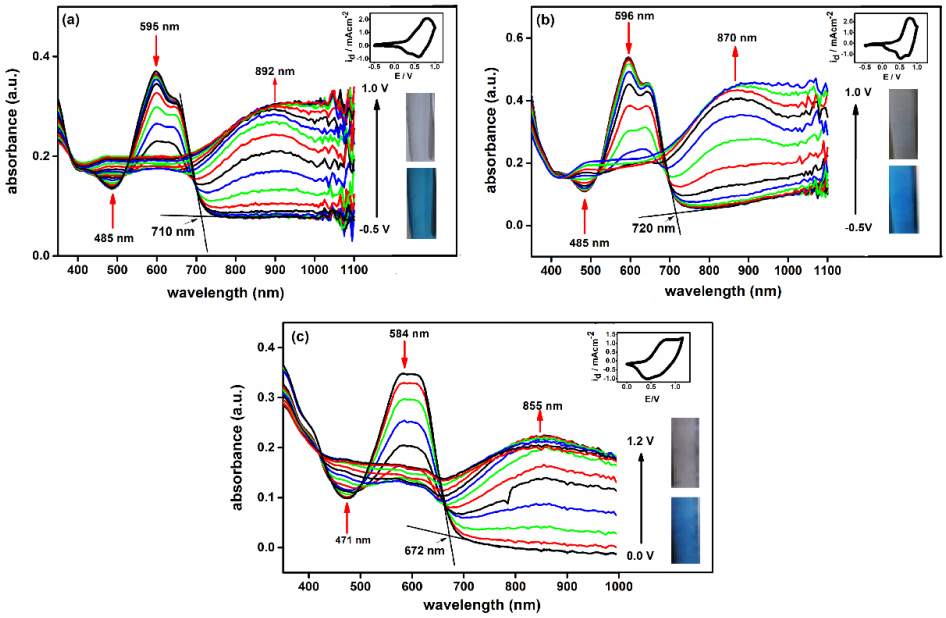


Figure 3. 19. Electronic absorption spectra of the polymers on ITO recorded in ACN containing 0.1 M $TBAPF_6$ as electrolyte between -0.5 and 1.0 V for **a) PM2**, **b) PM3** and between 0.0 and 1.2 V for **c) PM4**. Insets: CVs of polymer films recorded during spectroelectrochemical changes.

Table 3. 4. Optical band gaps of the polymers.

Polymers	λ_{max} (nm)	λ_{max}^{onset} (nm)	E_g^{opt} (eV)
PM2	595	710	1.75
PM3	596	720	1.72
PM4	584	672	1.84

The appearance of new bands indicates the formation of charge carries during p- doping of polymer films on the polymer backbone. The CVs recorded during in-situ spectroelectrochemical measurements are also given in the insets of Figure 3.19 a-c, to clarify existence of doping and dedoping processes for the polymer films. These changes in the electronic absorption spectra observed during anodic scans were also accompanied by color change from deep blue to light grey as shown in Table 3. 5, indicating that all polymer films exhibit similar electrochromic behavior irrespective of substituents and/or linkage site. It is important to note that, although all polymer films exhibit reversible reduction peaks which might be due to n-doping of polymer films, no appreciable color change was noted during in-situ cathodic scans.

The optical band gap (E_g^{opt}) values of polymer films deposited on ITO via constant potential electrolysis at + 1.20 V were also determined from the onsets of low energy end of π–π* transitions in their neutral absorption spectra and the results are depicted in Table 3. 4. It was found that **PM4** has slightly higher E_g value (1.84 eV) as compared to **PM2** and **PM3** (1.75 and 1.72 eV, repectively). Although these values are found to be higher than that of E_g values obtained fom CV results, the changes for the three polymers follow the same trend (i.e E_g(**PM4**)>E_g(**PM2**)>E_g(**PM3**)). The reason for this trend, E_g value of 2,7 linked carbozole derivative being greater than 3,6-linked carbazole derivatives might be explained in terms of planarity and substituent effects.

In fact, lack of vibronic features in the electronic absorption spectrum of **PM4** might be attributed to its low planarization due to large dihedral angles which decreases delocalization.[55] In 3,6-linked carbazoles, N atom of carbazole unit is at the para position with respect to donor acceptor linkage site which enhances electron donating ability of 3,6-carbazoles as it is already observed from the red shifts in the electronic absorption spectra of monomers. Furthermore, conjugation breaks appear in the middle of the carbazole units in 3,6- carbazole which results in a robust coplanar structure with a low oxidation potential and low E_g.[76] The slightly lower E_g of **PM3** as compared to **PM2** might be due to substituent effect, C_2H_5 group being better electron donating substituent than CH_3 group.

As it is already discussed in part 3.2.2.1 all three monomers have two reversible oxidation peaks together with one irreversible oxidation and one reversible reduction peaks. Due to similarities in the DPV of the **A2** with DPV of monomers, it is thought that reversible oxidation reduction peaks are originating from **A2** unit. To get more insight and to get stronger proof for this suggestion, **M3** was oxidized using a chemical oxidizing agent, $SbCl_5$. For this purpose, drop wise addition of dilute $SbCl_5$ solution in DCM to solution was monitored by recording the electronic absorption spectra after each drop addition of $SbCl_5$ solution and the changes are given in Figure 3. 20. a. The changes in the electronic absorption spectra recorded during the chemical oxidation of **M3** revealed that two high energy bands at 335 nm and 426 nm intensify and low energy ICT band loses intensity together with formation of three new bands at 496 nm, 926 nm and 1043 nm during the chemical oxidation. Two of the newly formed bands in the near IR region of electromagnetic spectrum indicate the formation of radical cation intermediates. Since changes resemble the changes that we obtained for **PM3** on ITO (Figure 3.19.b) we tried chemical oxidation of **PM3** in solution using the same chemical oxidizing agent. For this purpose we tried to dissolve **PM3** in several solvents and we found that it is partially soluble in o-dichlorobenzene. Thus soluble part of **PM3** in o-dichlorobenzene is titrated

with $SbCl_5$ solution and the changes recorded during the oxidation are given in Figure 3.20 b. Comparison of Figure 3.20 a and b revealed that not only the absorption bands present in the neutral form of **PM3** are red shifted due to increased conjugation upon polymer formation but also the number and position of newly formed bands also changed. One of the most pronounced differences was the formation of a broad band centered at 817 nm instead of two newly formed bands during oxidation of **M3**. This difference is mainly because of the different hosts for the radical cation intermediates, i.e. polymer chains (**PM3**) and small **M3** molecule. The changes observed during oxidation of **PM3** film is also included into Figure 3.20 for comparison sake (Figure 3.20. c). Comparison of changes in the absorption spectra of **PM3** in o-dichlorobenzene with **PM3** on ITO revealed same general feature, except for about 10 nm red shift of all absorption bands of **PM3** on ITO. The reason for this red shift might be explained due to increased π stacking for the solid polymer film. To present the differences in the electronic absorption spectra of **M3**, **PM3** in solution and **PM3** thin film both in their neutral and oxidized forms are also given in Figure 3.20.d.

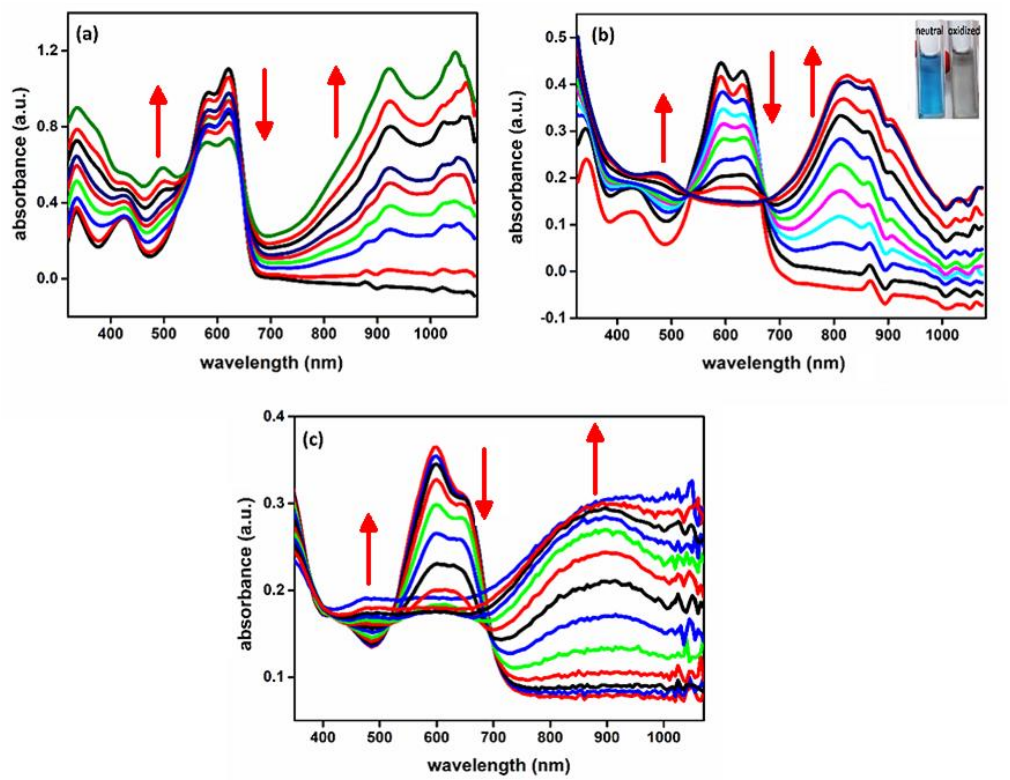


Figure 3. 20. Changes in the electronic absorption spectrum of **(a) M3** during controlled oxidation with $SbCl_5$ in DCM **(b) PM3** during controlled oxidation with $SbCl_5$ in o-dichlorobenzene **(c) PM3** during electrochemical oxidation on ITO in 0.1 M $TBAPF_6$/ACN.

3.3.8. Kinetic Studies of the Polymers

Since optical contrast and switching times are among the most importont factors for electrochromic device applications, optical contrast and switching times of polymeric films on ITO were also investigated under square wave input of determinated potential ranges in 1, 3, 5 and 10 s intervals by monitoring the transmittance and the kinetic responses of the film at given wavelengths in **Table 3.5.**

As seen from Figure 3.21. a, **PM2** shows a reversible response within the applied range of applied potentials pulses (-0.5 V and +1.0 V) with a response time of 1.2 s (at 650 nm) and 0.9 s (at 850 nm) at 95 % of the maximum transmittance. Optical contrast (Δ%T) values were found to be 22 % and 27 % at 650 nm and 850 nm, respectively. For **PM3,** the response time of 0.27 s at 95 % of the maximum transmittance and Δ%T was 16 % at 595. In the case of **PM4** due to dissolution of polymer film in ACN these values were not evaluated. Furthermore, due to its importance for electrochromic applications their coloration efficiencies (CE) were also evaluated. **PM2** has CE of 307 and 423 cm^2/C at 650 and 850 nm, respectively. CE for **PM3** was found to be 500 cm^2/C at 595nm. These values are also tabulated in Table 3.5 for comparison reason. As seen from theTable 3.5 **PM3** has the highest CE and the shortest switching time among the polymer films synthesized in this work.

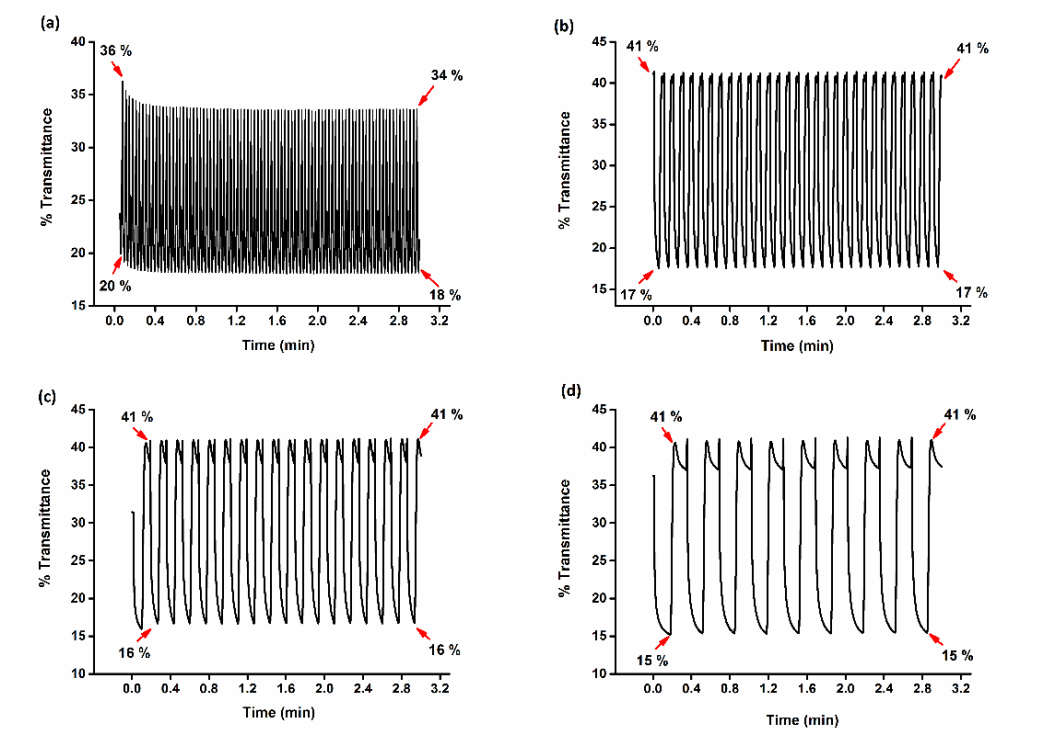


Figure 3. 21. Chronoabsorptometry experiments for **PM2** on ITO in 0.1 M $TBABF_4$/ACN while the polymer was switched between -0.5 and 1.0 V with a switch time of (a) 1, (b) 3, (c) 5 and (d) 10 s at 650 nm.

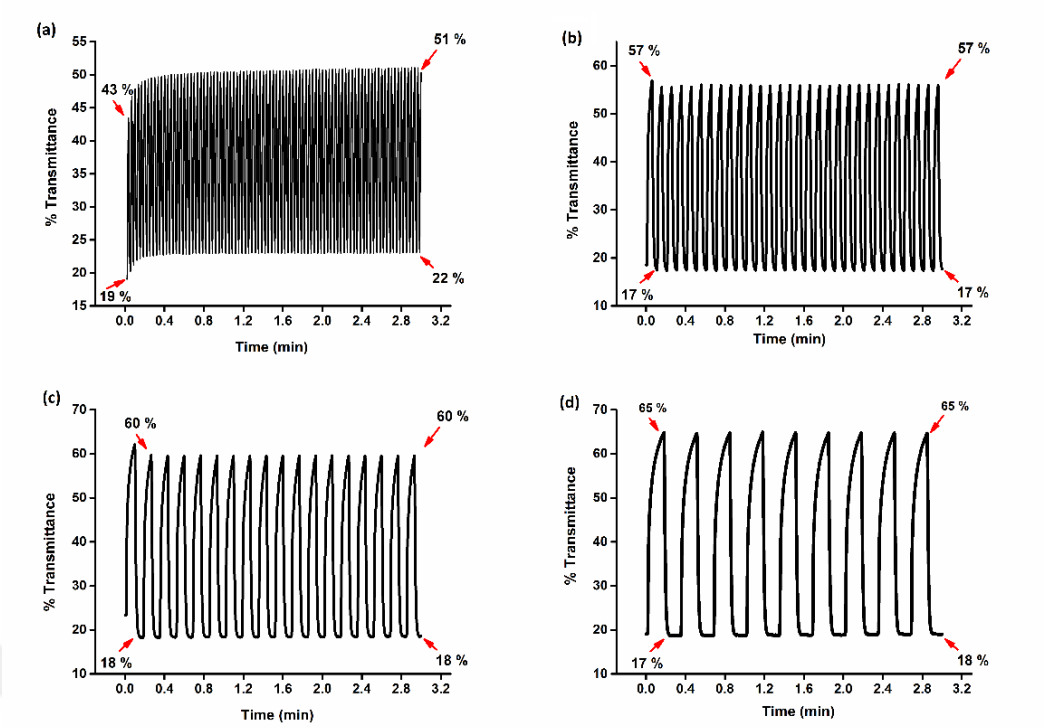


Figure 3. 22. Chronoabsorptometry experiments for **PM2** on ITO in 0.1 M $TBABF_4$/ACN while the polymer was switched between -0.5 and 1.0 V with a switch time of (a) 1, (b) 3, (c) 5 and (d) 10 s at 850 nm.

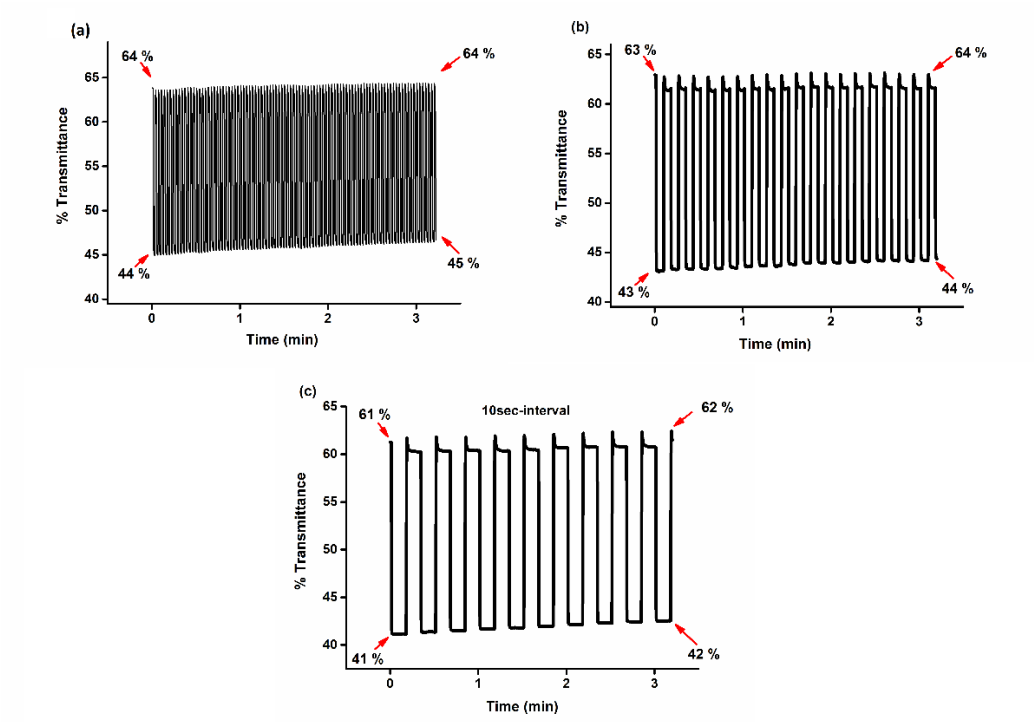
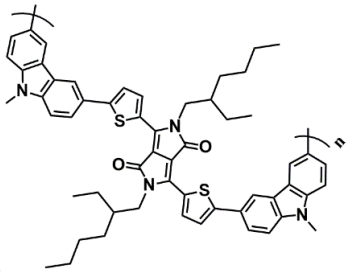
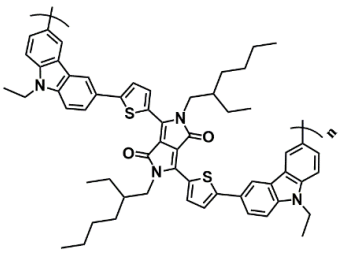
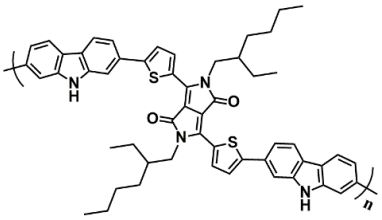


Figure 3. 23. Chronoabsorptometry experiments for **PM3** on ITO in 0.1 M $TBABF_4$/ACN while the polymer was switched between -0.5 and 1.0 V with a switch time of (a) 1, (b) 5, and (c) 10 s at 595 nm.

Table 3. 5. CE, switching time and colors of the polymers

Polymer	λ_{max} (nm)	CE ($cm^2.C^{-1}$)	ST (s)	% T	Neutral color	Oxidized color
PM2 	**650**	**307**	**1.2**	**25**		
	850	**423**	**0.9**	**30**		
PM3 	**595**	**500**	**0.3**	**20**		
PM4 	-	-	-	-		

3.3.9. FTIR Results of the Polymers

To get insight into differences between monomer and polymer films, FTIR spectrums were taken and are shown in Figure 3.24. In the FTIR spectra of polymers, two main characteristics are seen. First one is the stretching due to DPP moiety. The characteristic peaks are observed at 2958 - 2853 cm^{-1} due to C-H alkyl stretching, 1648 cm^{-1} due to C=O group[77] which is more intense than the peak at 1548 due to symmetrical C=C stretching in DPP unit. The peaks observed in the range of 1400-1472 cm^{-1} are due to methyl and methylene stretching, 1190 and 1364 due to C-N stretching, 921 and 872 $cm^{-1}$are as a result of in plane and out of plane deformation of five membered aromatic ring.[78] The second main stretching are due carbazole moiety at 3014 - 3075 cm^{-1} for aromatic C-H stretching, 1597 cm^{-1} for asymmetrical aromatic C=C stretching, 1515-1496 for aromatic C-C stretching, 1364, 1190 cm^{-1} for C-N stretching, 1329 cm^{-1} for C-C inter ring stretching, 1073-1300 for aromatic C-H in plane bending.[79] The peaks in the range of 621 to 726 are out of plane ring bending. The peaks from 741 to 840 cm^{-1} region indicate the substituted aromatic ring of carbazole and inplane C–H deformation.[80] In this region, the existence of peaks at 1019 and 839-796 cm^{-1} corresponds to parasubstitution that stands for 3,6- carbazole and the peak at 761-743 cm^{-1} is due to 1,2 disubstituted benzene ring.[81] After electrochemical polymerization of the monomers, the peaks at around 761-743 cm^{-1} disappears. However, the peaks at 839-796 and 1019 $cm^{-1}$are still present indicating the presence of 1,2,4-trisubstituted benzene rings. These changes confirm that 3,6 -linked monomer (**M2**) is polymerized via C-3 carbon atom and 2,7-linked monomer (**M4**) polymerized via C-2 carbon atoms of carbazole moiety. The peak due to N-H stretching appears at 3406 cm^{-1} for **M4** which is not present in the spectrum of **M2** due to presence of methyl group instead of hydrogen atom on the nitrogen atom.

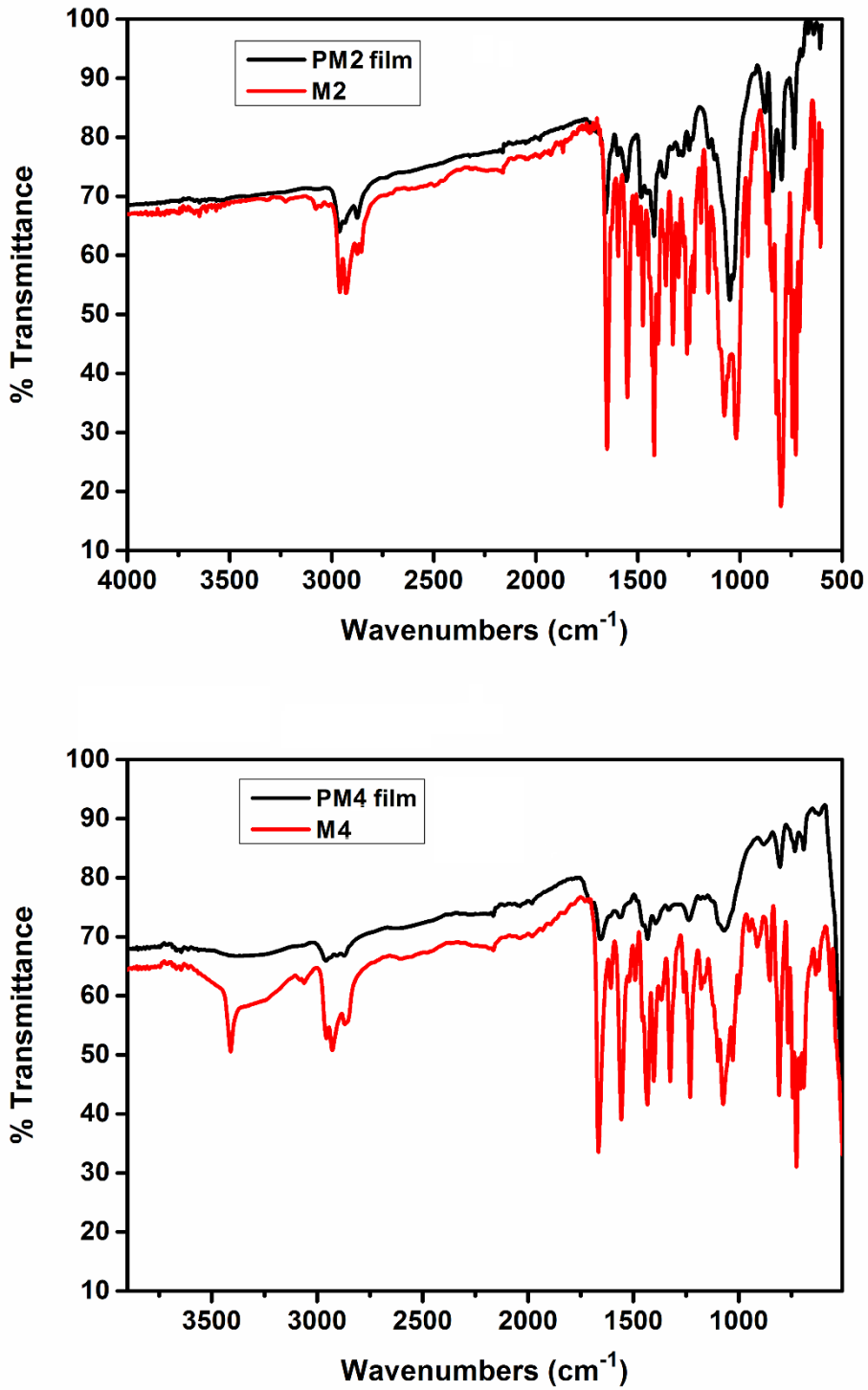


Figure 3. 24. FTIR spectra of **(a)** and **(b) M2** and **PM2, (c)** and **(d) M8** and **PM8**.

CHAPTER 4

CONCLUSIONS

In this study, four new donor-acceptor type monomers were synthesized and the differences of the corresponding polymers were analyzed. 2,7 and 3,6-linked carbazole derivatives were used as a donor unit and TPD and DPP units were used as an acceptor unit. The differences were expected to be caused by different substitution sites of carbazole, alkyl chain attached to the nitrogen atom and thiophene flanking units of DPP. All monomers were polymerized in DCM-BFEE medium successfully. It was observed that, the polymers containing DPP and 3,6 and 2,7-linked carbazoles show similar color change between blue and transmissive grey; however, the polymer containing TPD and 3,6-substituted carbazole has a tendency to change their color from yellow to light brown. Moreover, optical and kinetic behaviors of the **PM2** and **PM3** were also investigated. According to these studies, **PM3** was found to have the highest CE and the lowest switching time at 595 nm. On the other hand, **PM2** was found to exhibit highest optical contrast value (% 42) at 850 nm.

The changes in the electronic absorption spectra of the polymer films were also investigated using in-situ spectroelectrochemical technique in $TBABF_4$/ACN. Both electrochemical and spectroelectrochemical results were used to elucidate E_g values of the polymer films. Band gap values of DPP containing polymers were found to be much lower (around 1.60 eV) than that of TPD containing polymer (E_g=2.70 eV) indicating that DPP is a stronger acceptor unit as compared to TPD. When the linkage site of carbazole unit was considered, it was found that 2,7-linked carbazole containing polymer **PM4** exhibits the lowest HOMO/LUMO levels and higher band gap as compared to 3,6-linked analogues. The differences were explained in terms of different electron donating ability of N atom, planarity and effective conjugation length.

REFERENCES

1) H. Shirakawa, E. J. Louis, A. G. MacDiarmid, C. K. Chiang and A. J. Heeger, *J. Chem. Soc. Chem. Commun.*, 1977, 578–580.

2) K. Gurunathan, A. V. Murugan, R. Marimuthu, U. Mulik and D. . Amalnerkar, *Mater. Chem. Phys.*, 1999, 61, 173–191.

3) L. Jan and A. Koster, *Device physics of donor / acceptor-blend solar cells*, 2007.

4) S. Günes, H. Neugebauer and N. S. Sariciftci, *Chem. Rev.*, 2007, 107, 1324–1338.

5) Y. Cheng, S.H. Yang and C. Hsu. *Chem. Rev*., 2009, 109, 5868–5923

6) P. Schilinsky, U. Asawapirom, U. Scherf, M. Biele and C. J. Brabec, *Chem. Mater.*, 2005, 17, 2175–2180.

7) J. L. Brédas, *J. Chem. Phys.*, 1985, 82, 3808-3811.

8) J. S. Lee, S. K. Son, S. Song, H. Kim, D. R. Lee, K. Kim, M. J. Ko, D. H. Choi, B. S. Kim and J. H. Cho, *Chem. Mater.*, 2012, 24, 1316–1323.

9) J. Roncali, *Chem. Rev.*, 1997, 97, 173–206.

10) H. T. Black, A. Dadvand, S. B. Liu, V. S. Ashby and D. F. Perepichka, *J. Mater. Chem. C*, 2013, 1, 260–267.

11) S. B. Darling and M. Sternberg, *J. Phys. Chem. B*, 2009, 113, 6215–6218.

12) I. Osaka, *Polym. J.*, 2014, 47, 18–2590.

13) M. Akbayrak, E. G. Cansu-Ergun and A. M. Önal, *Des. Monomers Polym.*, 2016, 19, 679–687.

14) J. Wu, W. Walukiewicz, K. M. Yu, J. W. Ager, E. E. Haller, H. Lu, W. J. Schaff, Y. Saito and Y. Nanishi, *Appl. Phys. Lett.*, 2002, 80, 3967–3969.

15) Thomas C. A., Donor-acceptor methods for band gap reduction in conjugated polymers: the role of electron rich donor heterocycles, University of Florida, 2002.

16) M. D. Earle, *J. Franklin Inst.*, 1951, 252, 95.

17) R. Kroon, D. A. Mengistie, D. Kiefer, J. Hynynen, J. D. Ryan, L. Yu and C. Müller, *Chem. Soc. Rev.*, 2016. DOI: 10.1039/c6cs00149a

18) A. J. Heeger, S. Kivelson, J. R. Schrieffer and W. P. Su, *Rev. Mod. Phys.*, 1988, 60, 781–850.

19) D. M. de Leeuw, M. M. J. Simenon, R. Brown and R. E. F. Einerhand, *Synth. Met.*, 1997, 87, 53–59.

20) Retrieved from http://hyperphysics.phy-astr.gsu.edu/hbase/solids/dope.html on April 18, 2014

21) M. Mueller, M. Fabretto, D. Evans, P. Hojati-Talemi, C. Gruber and P. Murphy, *Polym.*, 2012, 53, 2146–2151.

22) J. Tahalyani, K. K. Rahangdale and B. K, *RSC Adv.*, 2016, 6, 69733–69742.

23) L. Beverina, G. a Pagani and M. Sassi, *Chem. Commun.*, 2014, 50, 5413–30.

24) N. K. Jangid, N. Chauhan, K. Meghwal and P. Bunjabi, *Res. J. Pharm. Biol. Chem. Sci.*, 2014, 5, 383–412.

25) P. Sengodu and A. D. Deshmukhb, *RSC Adv.*, 2015, 5, 42109-42130

26) A. J. Heeger, *Chem. Soc. Rev.*, 2010, 39, 2354-2371.

27) F. C. Spano and C. Silva, *Annu. Rev. Phys. Chem.*, 2014, 65, 477–500.

28) A. A. Argun, P. H. Aubert, B. C. Thompson, I. Schwendeman, C. L. Gaupp, J. Hwang, N. J. Pinto, D. B. Tanner, A. G. MacDiarmid and J. R. Reynolds, *Chem. Mater.*, 2004, 16, 4401–4412.

29) R. J. Mortimer, D. R. Rosseinsky and P. M. S. Monk, *Electrochromic Mater. Devices*, 2015, 77, 1–638.

30) G. E. Gunbas, A. Durmus and L. Toppare, *Adv. Funct. Mater.*, 2008, 18, 2026–2030.

31) Retrieved from https://www.mcgill.ca/chemistry/channels/event/csacs-seminar-john-reynolds-color-conjugated-polymers-electrochromism-and-photovoltaics-247965 on August 8, 2016

32) L. Beverina, G. Pagani and M. Sassi, *Chem. Commun.*, 2014, 50, 5413–30.

33) T. Okada, T. Ogata and M. Ueda, *Macromol. Rapid Commun.*, 1996, 29, 7645–7650.

34) R. H. Baughman, J. L. Brédas, R. R. Chance, R. L. Elsenbaumer and L. W. Shacklette, *Chem. Rev.*, 1982, 209–222.

35) J. Roncali, *Chem. Rev.*, 1992, 92, 711–738.

36) M. Gvozdenovic, B. Jugovic, J. Stevanovic and B. Grgur, *Hem. Ind.*, 2014, 68, 673–684.

37) K. M. Molapo, P. M. Ndangili, R. F. Ajayi, G. Mbambisa, S. M. Mailu, N. Njomo, M. Masikini, P. Baker and E. I. Iwuoha, *Int. J. Electrochem. Sci.*, 2012, 7, 11859–11875.

38) U. Christmann and R. Vilar, *Angew. Chemie - Int. Ed.*, 2005, 44, 366–374.

39) N. Miyaura and A. Suzuki, *Chem. Rev.*, 1995, 95, 2457–2483.

40) R. Martin and S. L. Buchwald, *Acc. Chem. Res.*, 2008, 41, 1461–1473.

41) K. M. llen, J. R. Reynolds and T. Masudar, Conjugated Polymers: A Practical Guide to Synthesis, Royal Society of Chemistry, 2014, 113.

42) J. Lia and A. C. Grimsdale, *Chem. Soc. Rev.*, 2010, 39, 2399–2410

43) N. Blouin and M. Leclerc, *Acc. Chem. Res.*, 2008, 41, 1–10.

44) J. V. Grazulevicius, P. Strohriegl, J. Pielichowski and K. Pielichowski, *Prog. Polym. Sci.*, 2003, 28, 1297–1353.

45) G. Zotti, G. Schiavon, S. Zecchin, J. F. Morin and M. Leclerc, *Macromolecules*, 2002, 35, 2122–2128.

46) P. Data, P. Pander, M. Lapkowski, A. Swist, J. Soloducho, R. R. Reghu and J. V. Grazulevicius, *Electrochim. Acta*, 2014, 128, 430–438.

47) Y. Zou, D. Gendron, R. Neagu-Plesu and M. Leclerc, *Macromolecules*, 2009, 42, 6361–6365.

48) Y. Zou, D. Gendron, A. Najari, Y. Tao and M. Leclerc, *Science*, 2009, 2891–2894.

49) E. Zhou, S. Yamakawa, K. Tajima, C. Yang and K. Hashimoto, *Chem. Mater.*, 2009, 21, 4055–4061.

50) G. Zhang, Y. Fu, L. Qiu and Z. Xie, *Polym*, 2012, 53, 4407–4412.

51) Y. Zou, A. Najari, P. Berrouard, S. Beaupre, B. R. Aïch, Y. Tao and M. Leclerc, *J. Am. Chem. Soc.*, 2010, 132, 5330–5331.

52) Y. Zhang, S. K. Hau, H. L. Yip, Y. Sun, O. Acton and A. K. Y. Jen, *Chem. Mater.*, 2010, 22, 2696–2698.

53) S. Wen, W. Cheng, P. Li, S. Yao, B. Xu, H. Li, Y. Gao, Z. Wang and W. Tian, *J. Polym. Sci. Part A Polym. Chem.*, 2012, 50, 3758–3766.

54) L. Huo, J. Hou, H. Y. Chen, S. Zhang, Y. Jiang, T. L. Chen and Y. Yang, *Macromolecules*, 2009, 42, 6564–6571.

55) C. Wang, C. J. Mueller, E. Gann, A. C. Y. Liu, M. Thelakkat and C. R. McNeill, *J. Mater. Chem. A*, 2016, 4, 3477–3486.

56) K. Narayanaswamy, Tiwari, I. Mondal, U. Pal, S. Niveditha, K. Bhanuprakash and S. P. Singh, *Phys Chem Chem Phys*, 2015, 17, 13710–13718.

57) W. Li, K. H. Hendriks, M. M. Wienk and R. A. J. Janssen, *Acc. Chem. Res.*, 2016, 49, 78–85.

58) M. Kaur and D. H. Choi, *Chem. Soc. Rev.*, 2015, 44, 58–77.

59) C. B. Nielsen, M. Turbiez and I. McCulloch, *Adv. Mater.*, 2013, 25, 1859–1880.

60) P. Camurlu, *RSC Adv.*, 2014, 4, 55832–55845.

61) L. Kong, Z. Wang, J. S. Zhao and J. Z. Xu, *Int. J. Electrochem. Sci.*, 2015, 10, 982–996.

62) P. M. Beaujuge and J. R. Reynolds, *Chem. Rev.*, 2010, 110, 268–320.

63) G. Nie, L. Wang and C. Liu, *J. Mater. Chem. C*, 2015, 3, 11318–11325.

64) Y. Yasutani, Y. Honsho, A. Saeki and S. Seki, *Synth. Met.*, 2012, 162, 1713–1721.

65) M. A. Uddin, T. Kim, S. Yum, H. Choi, S. Hwang, J. Y. Kim and H. Y. Woo, *Curr. Appl. Phys.*, 2015, 15, 654–661.

66) G. Wiosna-Salyga, M. Gora, M. Zagorska, P. Toman, B. Luszczynska, J. Pfleger, I. Glowacki, J. Ulanski, J. Mieczkowski and A. Pron, *RSC Adv.*, 2015, 5, 59616–59629.

67) H. Bürckstümmer, A. Weissenstein, D. Bialas and F. Würthner, *J. Org. Chem.*, 2011, 76, 2426–2432.

68) W.S. Shin, S.C. Kim, S.-J.Lee, H.S. Jeon, M.-K. Kim, B.V.K. Naidu, S.-H. Jin, J.-K. Lee, J.W. Lee and Y.S. Gal, *J. Polym. Sci. Part A: Polym. Chem.*, 2007, 45, 1394.

69) K. Dhanalakshmi, R. Saraswathi, J. Mater. Sci., 2001, 36, 4107-4115.

70) G. Sönmez, I. Schwendeman, P. Schottland, K. Zong and J. R. Reynolds, *Macromolecules*, 2003, 36, 639–647.

71) E. G. Cansu-Ergun and A. Cihaner, *J. Electroanal. Chem.*, 2013, 707, 78–84.

72) H. Yu, S. Shao, L. Yan, H. Meng, Y. He, C. Yao, P. Xu, X. Zhang, W. Hu and W. Huang, *J. Mater. Chem. C*, 2016, 4, 2269–2273.

73) G. Nie, H. Yang, S. Wang and X. Li, *Crit. Rev. Solid State Mater. Sci.*, 2011, 36, 209–228.

74) S. Chen, B. Sun, W. Hong, Z. Yan, H. Aziz, Y. Meng, J. Hollinger, D. S. Seferos and Y. Li, *J. Mater. Chem. C*, 2014, **2**, 1683-1690.

75) O. Kwon, J. Jo, B. Walker, G. C. Bazan and J. H. Seo, *J. Mater. Chem. A*, 2013, 1, 7118–7124.

76) J. Kim, Y. S. Kwon, W. S. Shin, S. J. Moon and T. Park, *Macromolecules*, 2011, 44, 1909–1919.

77) K. Zhang, New Conjugated PolymersBased on Benzodifuranone and Diketopyrrolopyrrole, Köln, 2010.

78) F. Alakhras and R. Holze, *J. Solid State Electrochem.*, 2008, 12, 81–94.

79) A. S. Sarac, S. A. M. Tofail, M. Serantoni, J. Henry, V. J. Cunnane and J. B. McMonagle, *Appl. Surf. Sci.*, 2004, 222, 148–165.

80) A. Zahoor, T. Qiu, J. Zhang and X. Li, *J. Mater. Sci.*, 2009, 44, 6054–6059.

81) T. Miyazaki, S. K. Kim and K. Hoshino, *Chem. Mater.*, 2006, 18, 5302–5311.

APPENDIX

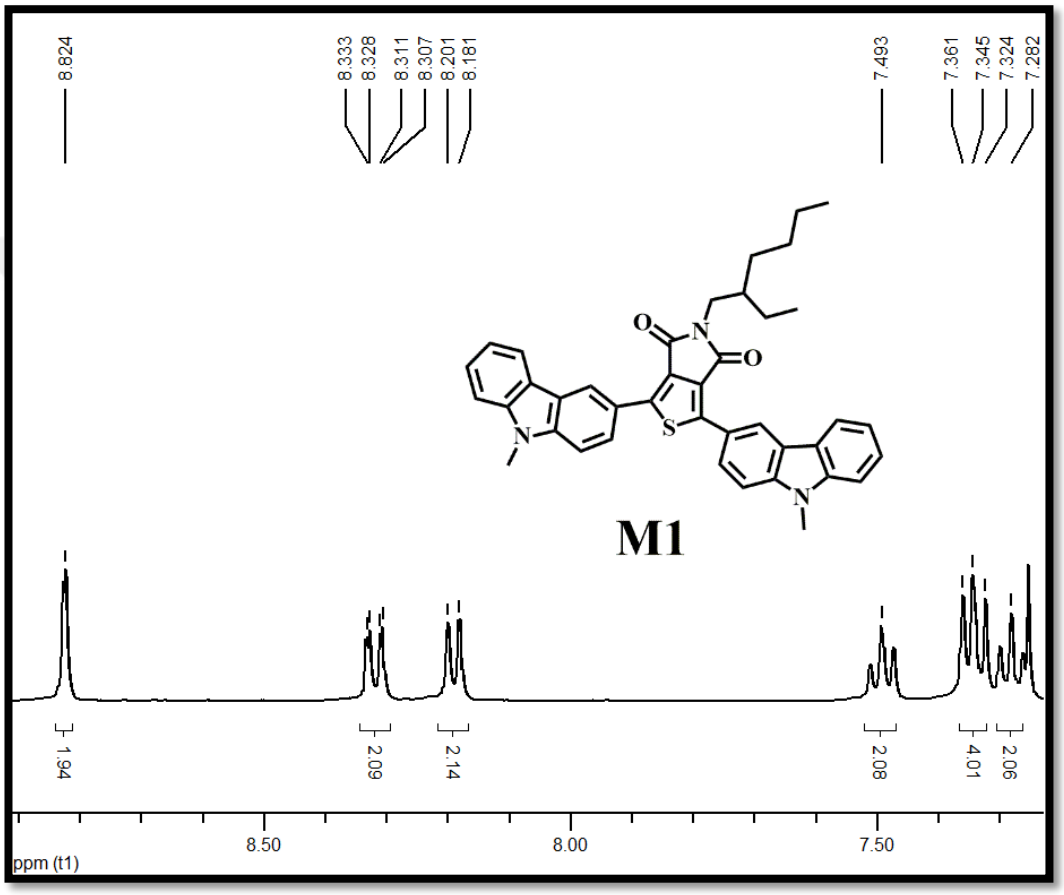


Figure A. 1. Aromatic region of ^{1}H NMR spectrum of **M1**.

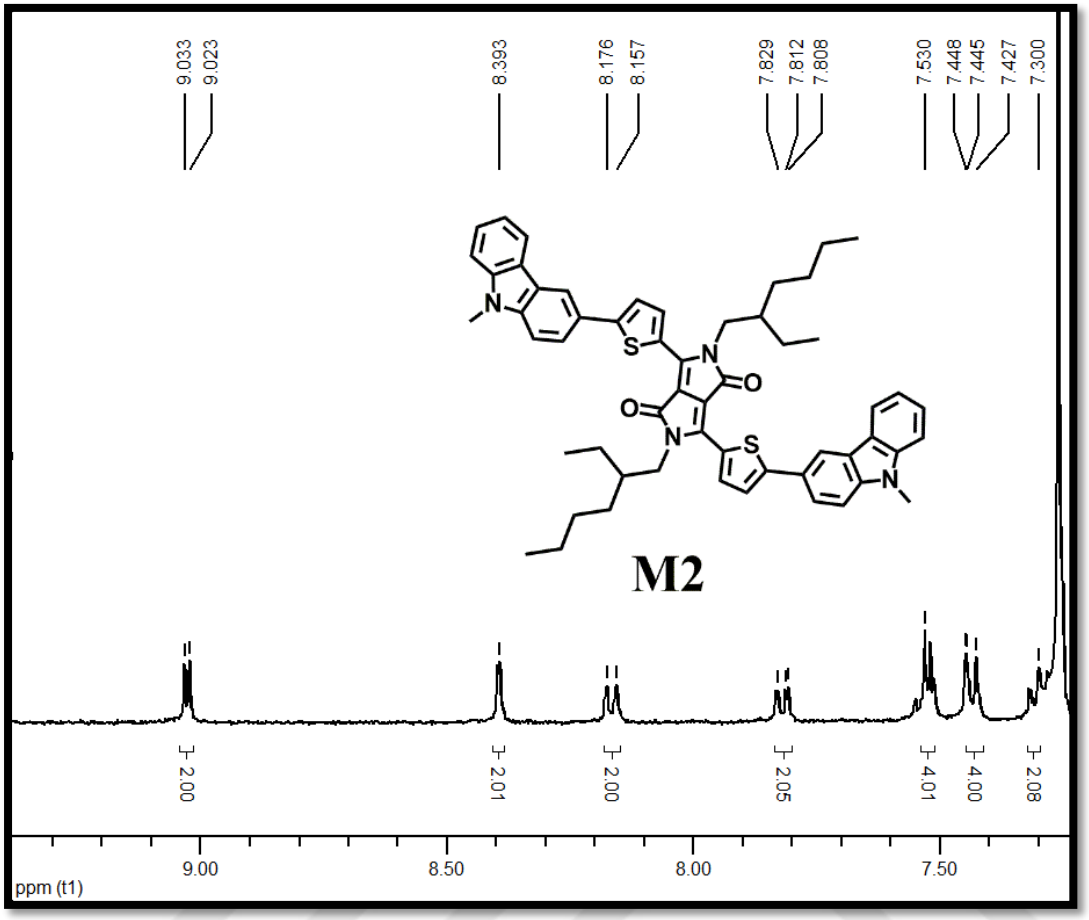


Figure A. 2. Aromatic region of ^{1}H NMR spectrum of **M2**.

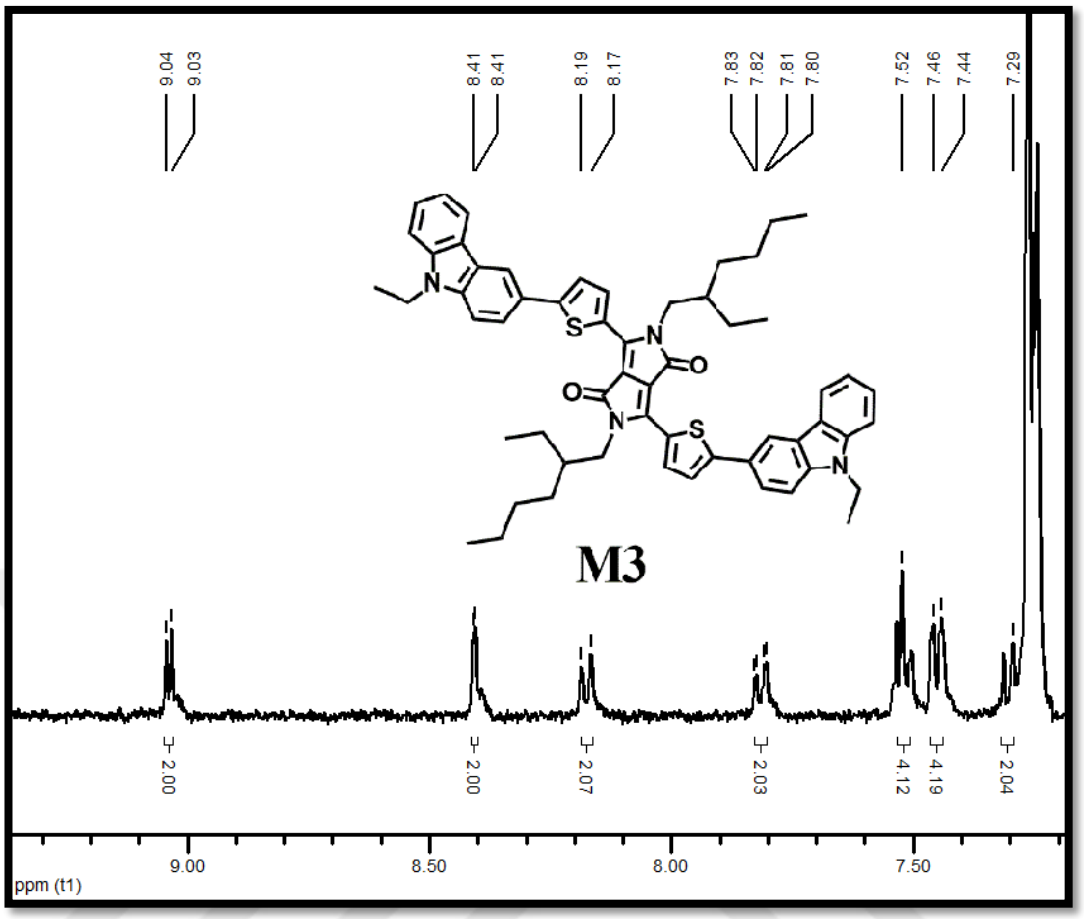


Figure A. 3. Aromatic region of ^{1}H NMR spectrum of **M3**.

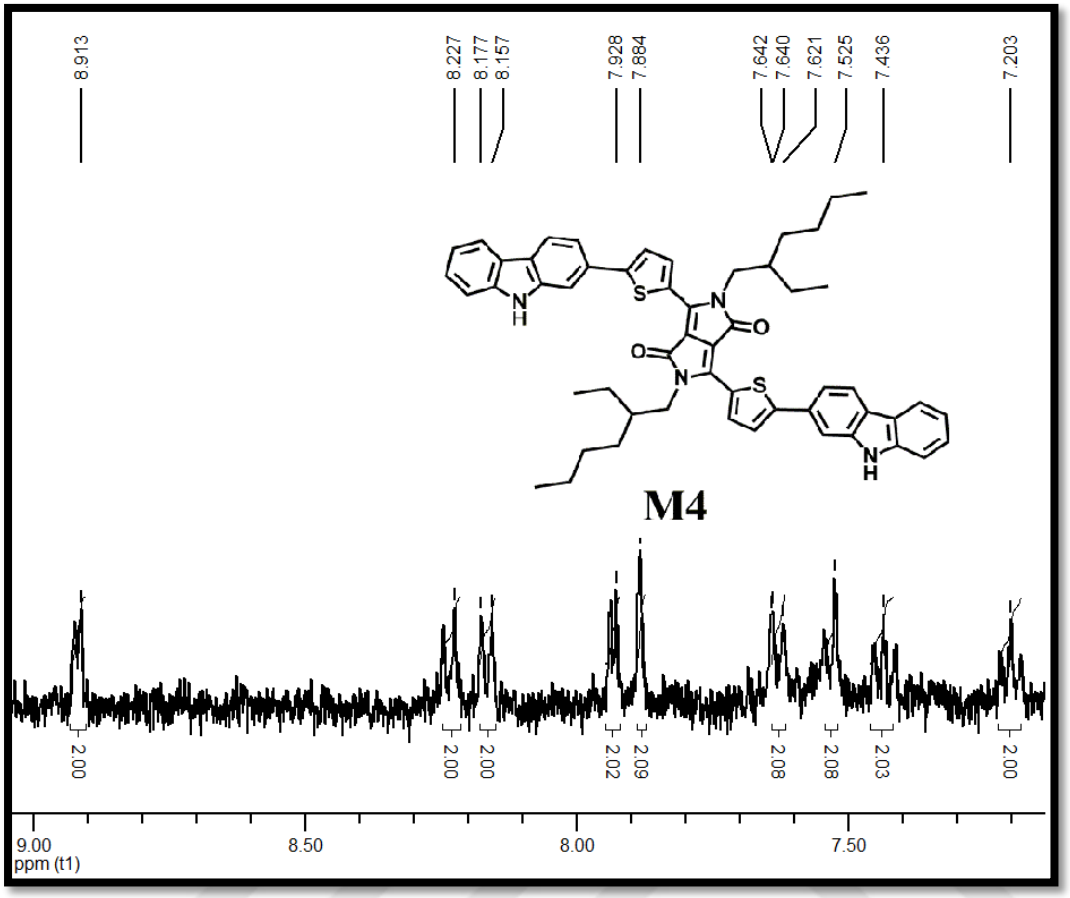


Figure A. 4. Aromatic region of ^{1}H NMR spectrum of **M4**.